CALCULATIONAL METHODS FOR LATTICE CELLS

J.R. ASKEW
UKAEA Reactor Group,
Atomic Energy Establishment,
Winfrith,
United Kingdom

1.1 INTRODUCTION

The basic equations governing the motion and reaction of neutrons in nuclear reactors are of a very simple form, despite the complexity of much of the underlying physics. Given the very large effort which has been devoted to the measurement of nuclear data - that is, the characterization of these physics processes, - it is in principle possible to model the behaviour of a reactor core and shield to a level of accuracy far beyond that usually encountered in engineering applications.

The development of digital computers, and systematic development of calculational techniques, has revolutionized reactor design in a comparatively short time, say 20 years. Experimental studies, which once involved a large outlay in time and money to explore variations in fuel pin size, pitch, etc and were followed by progressive increases of scale of plant, have now been reduced to relatively specific and highly sophisticated experiments to confirm specific performance predictions, often those with safety implications.

The cost of experimentation, partly associated with the stringent safety standards adopted in its conduct, is clearly one of the factors encouraging improved modelling. So, at the other end of the scale, is the large capital cost of the finished power station.

As computing capabilities have improved, it has proved possible to produce more and more basic models, which have a wider range of validity. For example, it is possible to use the same models for reactors with different moderators. At the current stage of development, direct simulation of all the processes involved in the reactor to the degree of accuracy required is not an economic proposition, and this is achieved by progressive synthesis of models for parts of the full space/angle/energy neutron behaviour.

The split between reactor and lattice calculations is one such simplification. Most reactors are constructed of repetitions of similar geometric units, the fuel elements, having broadly similar properties. Thus the provision of detailed predictions of their behaviour is an important step towards overall modelling. We shall be dealing with these lattice methods in this series of lectures, but will refer back from time to time to their relationship with overall reactor calculation.

The lattice cell is itself composed of somewhat similar sub-units, the fuel pins, and will itself often rely upon a further break down of modelling. Construction of a good model depends upon the identification, on physical and mathematical grounds, of the most helpful division of the calculation at this level. Figure 1 shows the type of sub-division adopted in the WIMS lattice code schemes which is characteristic of most subsequent models. We shall deal in turn with the problems is each part of the calculation.

1.2 CHARACTERISTICS OF THE UNDERLYING PHYSICAL PROCESS

From the modelling point of view we can distinguish three basic regimes of neutron energy in which our preoccupations will be different.

(i) The Fast Region E>100 KeV

Neutrons from fission are born in this energy range. It is characterized by a wide diversity of possible neutron reactions, including sharp energy variations of reactions probability at thresholds, for example of fast fission in Uranium-238. Scattering is often highly anisotropic, even in the centre-of-mass frame of reference. Cross sections are usually fairly small - that is, neutrons travel longer distances between collisions than is the case at lower energies - and the representation of geometric details is correspondingly less important.

(ii) The Resonance Region 100 KeV > E > 4 eV

In this range the light nuclides tend to have constant cross-sections dominated by potential scattering. Intermediate and heavy nuclides exhibit resonances in which capture and fission cross-sections reach high values over small energy ranges and are temperature dependent due to the relative motion of neutron and nuclide (Doppler Broadening). Given these rapid changes, or discontinuities, of cross-section respectively in energy and space the modelling problem is at its most difficult. Because of the high cross-sections many of the effects are of short range.

(iii) The Thermal Region 4 eV > E

Here thermal motion of the light nuclides has a dominant effect upon neutron behaviour. The width of resonances is greater compared to possible energy change per collision, and in this sense cross-sections can be considered to be more slowly varying.

1.3 THE BOLTZMANN EQUATION

Neutrons may be considered to travel in straight lines in between events ("collisons") which are relatively localized in space and which can result in changes of direction and energy. The transmutation or displacement of nuclii is on such a small scale that the properties of the medium are essentially independent of the neutron flux, and the overall behaviour of the neutron flux is therefore described by the Boltzmann equation.

$$\frac{dN}{ds} + \Sigma_T N = Q$$

where $N = N(\underline{r},E,\underline{\Omega})$ is the neutron flux

$\Sigma_t = \Sigma_t(\underline{r},E)$ the total cross-section (isotropic)

$Q = Q(\underline{r},E,\underline{\Omega})$ is the neutron source

$$= \iint \Sigma(E'\to E,\underline{\Omega}'\to\underline{\Omega})\ N(\underline{r},E',\underline{\Omega}')\ dE'\ d'\underline{\Omega}'$$

Σ = transfer cross-section for all processes

s = space co-ordinate in direction $\underline{\Omega}$

Note that the total cross-section is related to the laboratory framework, as is the transfer cross-section. Motion of the target nucleus thus has to be allowed for in determining the constants in the equations, rather than appearing explicitly in the equations. The most obvious instance is the Doppler effect in which a resonance, in which the reaction probability is fixed in terms of the relative velocity of incident neutron and target nucleus, becomes temperature dependent in our formulation and exhibits an apparent spread.

It must not be assumed that because this equation is a good description of neutron motion it will also hold exactly under approximate conditions. In particular, condensation to group form in energy may be seen to introduce problems even if we know the exact solution. For if we define

$$\bar{N}(\underline{r},g,\underline{\Omega}) = \int_{\Delta E} N(\underline{r},E,\underline{\Omega})\ dE$$

where g denotes group of width ΔE.

we see that for consistency we require

$$\int_{\Delta E} \Sigma_t(E)\ N(\underline{r},E,\underline{\Omega}) = \bar{\Sigma}_t\ \bar{N}(\underline{r},g,\underline{\Omega})$$

and thus $\bar{\Sigma}_t = \bar{\Sigma}_t(\underline{r},\underline{\Omega})$ in general, unlike its point energy form which is independent of $\underline{\Omega}$. Particular care has to be taken in generalizing from deductions made in one energy group.

An exactly similar problem arises in the representation of scattering, in that transfers due to a genuinely isotropic scattering process may become anisotropic in group form. Elastic scatter conforms to an angle/energy law, and of ocurse is not isotropic in the group to group form, but highly directional. This is especially easy to overlook in spherical harmonics expansions of the equation. Treatment of these effects is most important in shielding and whole reactor calculations. In lattice calculations the problems are more usually introduced in attempting to simplify the equation in some way.

1.4 TRANSPORT CORRECTIONS

The most important practical simplifications lie in the treatment of scattering, to reduce it to a simpler, usually isotropic form. The right-hand side of the Boltzmann equation contains scattering terms of the form (dropping the spatial co-ordinate $\underline{r}$).

$$\iint \Sigma_s(E'\to E,\underline{\Omega}'\to\underline{\Omega})\ N(E',\underline{\Omega}')\ dE'\ d\underline{\Omega}'$$

and the aim is to relate these to the left-hand side term

$$\Sigma_t(E)\ N(E,\underline{\Omega})$$

in an approximate way. This depends upon some knowledge of the angular flux. The standard treatment is to expand the scattering cross-section in spherical harmonics

$$\Sigma_s(E'\to E,\underline{\Omega}'\to\underline{\Omega}) = \sum_{\ell} \Sigma_{e\ell}(E'\to E)\ P_\ell(\mu)$$

where

$\mu = \underline{\Omega}.\underline{\Omega}'$.

and further by the addition theorem for spherical harmonics to

$$P_\ell(\mu) = \sum_{m=-\ell}^{+\ell} P_{\ell m}(\underline{\Omega})\, P_{\ell m}(\underline{\Omega}')^*$$

Thus if the angular flux N is also expanded in spherical harmonics series in terms of $\underline{\Omega}$.

$$N(E',\underline{\Omega}') = \sum_{\ell=0}^{\infty} \sum_{m=-\ell}^{+\ell} \phi_{\ell m}(E')\, P_{\ell m}(\underline{\Omega}')$$

and the orthogonality relationship used to simplify the result. Limiting the expansion to the lowest orders, our source term becomes

$$\Sigma_o(E'\to E)\,\phi_o(E') + 1/3\,\Sigma_1(E'\to E)\,\phi_1(E').\underline{\Omega}$$

and we can relate it to the LHS

$$\Sigma_t(E)\left\{\phi_o(E') + \phi_1(E).\underline{\Omega}\right\}$$

by equating appropriate moments.

Two main assumptions are made:-

(1) The diagonal approximation

$$\Sigma_1(E'\to E)\,\phi_1(E') = \Sigma_1(E)\,\phi_1(E)$$

hence

$$\Sigma_{tr} = \Sigma_t - 1/3\,\Sigma_1$$

(2) The row sum

$1/3\ \Sigma_1(E'\to E)\,\phi_1(E')/\phi_1(E)$ is evaluated and subtracted from $\Sigma_t(E)$. This depends upon an orginal guess or calculation of the P_1 flux moment.

These approximations have proved to be broadly adequate for many purposes, particularly for the calculation of leadage in which only low order movements are significant. For lattice cell calculations. However it must be recognized that a very high order expansion will be needed to represent the angle/energy relationship in scattering (which, for a single nuclide, has a δ-function form) and that low order expansions may be misleading.

2. COLLISION PROBABILITY FORMULATIONS

For many purposes it is convenient to use the integral form of the neutron transport equation.

Collisons at $(\underline{r},E) = \Sigma_t(\underline{r},E)\,\phi(\underline{r},E)$

$$= \frac{1}{4\pi} P(\underline{r}'\to\underline{r},E)\,\phi(\underline{r}',E,-\underline{\Omega})\,d\underline{r}\,d\underline{\Omega}$$

$P(\underline{r}\to\underline{r})$ represents the probability that a neutron born at $\underline{r}$ and aimed in the appropriate direction, will have its next collision at $\underline{r}$.

This formulation is especially convenient when the emission of neutrons may be regarded as isotropic, and does not vary too rapidly in space. In this case we can integrate the probability over spatial zones such that

$$\text{Collisions in volume at } J = \Sigma_J V_J \phi_J = \sum_I Q_I V_i P(I\to J)$$

where P (I→J) is the probability that neutrons born uniformly in volume I will have their next collision in region J.

This probability may be determined by numerical integration along a mesh of lines distributed uniformly in space and angle. Along a line intersecting I and J in intercepts ℓ_I and ℓ_J we see that the number of neutrons colliding in J is:

$$\frac{Q_I}{\Sigma_I}(1-e^{-\Sigma_I \ell_I})\,e^{-\bar{\Sigma}\bar{L}}\,(1-e^{-\Sigma_J \ell_J})$$

where $\bar{\Sigma}\bar{L}$ is the distance between the surfaces of I and J expressed in mean free paths. As the number of neutrons in an elementary volume about the time is $Q_I\,\ell_i\,\delta S$ it will readily be seen that

along each line - and thus for the integral over all lines - a reciprocal relationship holds

$$\Sigma_I V_P P(I \to J) = \Sigma_J V_J P(J \to I)$$

The total escape probability from a non-re-entrant region, I, may be determined by integration over all families of lines in all directions.

$$P_{escape} = \frac{\iint \frac{Q}{\Sigma} (1-e^{-\Sigma \ell}) \, d S \, d \underline{\Omega}}{\iint Q \, \ell \, d S \, d \underline{\Omega}}$$

when d S is the element of projected surface. It will be seen that in the limit as $\Sigma \to \infty$.

$$P_{escape} \longrightarrow \frac{1}{\Sigma \bar{\ell}} \quad ; \quad \bar{\ell} = \frac{4 \times \text{Volume}}{\text{Surface Area}}$$

where $\bar{\ell}$ is the mean chord length of the body. Using this fact we may extend our reciprocity relationship by considering one region to be black

$$\Sigma_I V_I P(I \to J) = \Sigma_I V_I P(I \to S) P(S \to J)$$

where S is the surface of region I

$$= \frac{\Sigma_I V_I}{\Sigma_I \frac{V_I}{\bar{\ell}}} P(S \to J)$$

$$= \Sigma_J V_J P(J \to S) \quad \text{by reciprocity}$$

Thus surface reciprocity may be deduced

$$S_I P(S \to J) = 4 \Sigma_J V_J P(J \to S)$$

and, incidentally, the neutron flux leaving I in this limit is isotropic outwards, Also of interest in some cases in the 'white limit' of the escape probability which is seen to depend upon the mean square chord

$$P_{\substack{escape \\ \Sigma \to 0}} = \frac{\frac{Q}{\Sigma} (\Sigma \ell - \frac{\Sigma^2 \ell^2}{2!} + ..) \, d S \, d \underline{\Omega}}{Q \, \ell \, d S \, d \underline{\Omega}}$$

$$= 1 - \frac{\Sigma \overline{\ell^2}}{\bar{\ell}}$$

The exponential form of the integral suggests that an appropriate rational approximation might be

$$P_{escape} = 1/1 + \Sigma \ell$$

which has the desired behaviour in the black limit.

Generalization of these formulae to cylindrical geometry is simplified by the fact that only projections of the generating lines into the plane need to be considered, and the exponential functions are replaced by Bickley-Naylor functions. Simple generating formulae are available for multi-annular systems. A great deal of ingenuity was devoted to obtaining simplified formulae for such geometries; the THESEUS model in WIMS being based upon such a calculational method. With modern computers the need for such approximations becomes significant.

3. REPRESENTATION OF RESONANCES

3.1 INTRODUCTION

Because of the rapid variation of cross-section with energy in the resonance region this represents one of the most difficult modelling problems for the reactor physicist. The resonance structure is of importance up to 10 KeV, even though the resonances cannot be resolved experimentally at such high energies. At the bottom end of the range the modelling is forced to change to accomodate thermalization effects. In the WIMS lattice codes the range 4 eV - 9.2 KeV is treated by a special model; in some other codes the resonances of Plutonium -240 and -242 at 1 eV are included in the resonance region, but this limits the modelling accuracy achievable, especially for high temperature reactor calculations.

Basic nuclear data for the most important nuclides are available as resonance parameters which are used in a multi-level formalism to reconstruct cross-sections and their variation with temperature (Doppler broadening). Where significant resonance structure is not resolved experimentally it is necessary to construct appropriate distributions of resonances by a statistical process. The uncertainly inherent in this is not very significant for thermal reactors.

Uranium-238, the most significant resonance absorber in thermal reactors, has resonance spaced at about 18 eV on average. The fissile nuclides have smaller resonances which are less distinct. The different nuclides compete with each other for neutron capture, and have to be represented together in a model - this requires a fairly fine mesh and of the order of 10^5 data points are needed to represent all resonances in the range required.

3.2 EXACT MODELS

The neutron flux varies rapidly with space, energy and angle in the resonance region of typical thermal reactors. Resonant absorbing nuclides in the centre of fuel pins are 'shielded' by those on the outside. It is practicable to solve problems of the order of 10^5 energy points for infinite homogeneous mixtures of absorbers and moderator 'exactly' (ie within the limitations imposed by the knowledge of the nuclear data). For realistic geometries of pins and fuel assemblies this is more difficult, and two options are available.

The first involves some simplification of the geometry; possibly by the use of collision probability methods implying spatially flat emission densities over spatial zones, sometimes restricting the representation of angular scatter to isotropic or P_1 approximations. This may be reasonable good but the errors introduced are difficult to quantify except for the simplest geometries (plate, single pin etc).

The second is the use of Monte Carlo techniques. In these the modelling can be as detailed as one wishes, but a degree of randomness remains in the results which can only be progressively reduced with increased computing cost. Such methods are generally inconvenient for design purposes because the stochastice element is inconvenient in studying the effects of small design changes, and the method is most used to validate approximate methods.

3.3 EQUIVALENCE MODELS

The earliest practical models for obtaining solutions to heterogeneous geometries were based upon equivalence principles. These may be simply illustrated for a two-region system of a fuel pin surrounded by moderator. If we assume the resonances narrow compared to the energy loss per collision in the moderator, and neglect moderation in the fuel, we may reasonably assume a spatially flat emission density Ψ in the moderator. Then at each energy we can assume

$$\Sigma_t^f(u)\, V^f \phi^f(u) = \psi^m(u)\, V^m P(m\to f, \Sigma_t^f)$$

where $\psi m(u)$ is the emission density slowly varying with lethargy

$\Sigma_t^f(u)$ is the total cross-section of the fuel

$\phi^f(u)$ is the scalar flux integrated over the fuel region

$P(m\to f, \Sigma_t^f)$ is the probability that a neutron 'born' in the moderator has its next collision in the fuel

V^m, V^f are volumes of moderator and fuel

by reciprocity

$$\Sigma_t^m V^m P(m\to f) = \Sigma_t^f V^f P(f\to m)$$

$$= \Sigma_t^f V^f (1-P(f\to f))$$

and

$$\phi^f(u) = \frac{\psi^m(v)}{\Sigma_t^m}(1-P(f\to f))$$

Use of the rational approximation

$$P(f\to f) = \frac{\Sigma_t^f \bar{\ell}}{a(\Sigma_t^f \bar{\ell}) + \Sigma_t^f \bar{\ell}} = \frac{\Sigma_t^f \bar{\ell}}{\bar{a} + \Sigma_t^f \bar{\ell}}$$

allows us to express the flux in a form familiar for homogeneous mixtures

$$\phi^f(u) = \frac{\psi^m(u)}{\Sigma_t^m}\left(\frac{\bar{a}}{\bar{a} + \Sigma_t^f \bar{\ell}}\right)$$

compared to

$$\phi^f(u) = \frac{\psi^m(u)}{\Sigma_t^m}\left(\frac{\Sigma_t^m}{\Sigma_t^m + \Sigma_t^f}\right)$$

The heterogeneous solution to the slowing down problem is thus, within the limitations of the rational approximation, similar in form to the homogeneous problem which can be solved exactly. The rational approximation is good as $\Sigma^f\bar{\ell}\to\infty$, $\bar{a}\to 1$ and hence is a good solution to the most difficult part of the modelling problem. The best value of $\bar{a}$ the BELL FACTOR may be obtained by fitting to explicit two region solutions. Its rational approximation, for example that due to Carlvik for cylidrical rods:-

$$P(f\to f) \simeq \frac{2\Sigma^f\bar{\ell}}{2+\Sigma^f\bar{\ell}} - \frac{\Sigma^f\bar{\ell}}{3+\Sigma^f\bar{\ell}}$$

$$\phi^f(u) \simeq \frac{\psi^m(u)}{\Sigma_t^m}\left[\frac{4}{2+\Sigma^f\bar{\ell}} - \frac{3}{3+\Sigma^f\bar{\ell}}\right]$$

which is related to the difference of two homogeneous solutions.

Following the analogy with homogeneous systems we see that, by choosing an energy internal (group) over which $\Psi(E)$ does not vary significantly - or, better, by ensuring that resonance absorptions are symmetric over the interval by placing dominant resonances in the middle of the internal, we can equivalence the homogeneous and heterogeneous RESONANCE INTEGRALS.

$$I = \Sigma_a \phi \, du = \frac{\Sigma_a \Sigma_p}{\Sigma_p+\Sigma_a} \, du$$

here Σp is the equivalent homogeneous scatter cross-section

$$\Sigma_p = \sum_{i \text{ in fuel}} n_i \lambda_i \sigma_{si} + \bar{a}/\bar{\ell}$$

it being found that suitable effective scatter cross-sections for fuel constituents such as Uranium and Oxygen can be deduced to fit both metal and oxide resonance integrals.

The last factor normally introduced in such a model is the DANCOFF FACTOR, which relates the fuel to fuel collision probability for an array of pins to that for a single pin. The computations are performed in the black limit $\Sigma f\to\infty$ and the Dancoff factor is defined as γ

$$\lim_{\Sigma^f\to\infty}\left[1-P(f\to f)\right]_{\text{array}} = \left[\frac{\gamma}{\Sigma_t^f\ell_{\text{pin}}}\right]$$

By consideration of the true form of the collision probabilities for arrays (given by Leslie) and use of the rational approximation given above it can be deduced, however, that the Bell factor is different for arrays. An approximate form is

$$a = a(\text{pin}) + 0.125\,(1-\gamma)$$

Refinements to treat the effect of cans, etc, may be obtained in a similar way and are described in the literature. Having obtained a resonance integral for a given fuel region by looking up the appropriate homogeneous equivalence, a consistent cross-section for the fuel region may be obtained. For if

$$I = \frac{\Sigma_a \Sigma_p}{\Sigma_p+\Sigma_a} \, du$$

$$\phi = \frac{\Sigma_p}{\Sigma_p+\Sigma_a} \, du = \left[\frac{\Sigma_p+\Sigma_a}{\Sigma_p+\Sigma_a} - \frac{\Sigma_a}{\Sigma_p+\Sigma_a}\right] du$$

$$= \Delta u - \frac{I}{\Sigma_p}$$

Hence

$$\Sigma_a^f = \frac{I}{\Delta u - I/\Sigma_p}$$

This step has often been neglected when preparing data for use in spatial solutions, with a typical error of 10% in Uranium-238 resonance events.

3.4 SUB-GROUP MODEL

This represents the next stage of sophistication in resonance representation. All resonances are replaced by weighted sums of fixed cross-sections. The weights may be regarded as equivalent to lethargy widths of 'sub-groups' over which the cross-sections are to apply. One way of obtaining sub-group data, which avoids unnecessary approximations, is to fit the weights to exact solutions for homogeneous mixture of absorber and hydrogen.

$$I_a = \int \frac{\Sigma_p+\Sigma_a}{\Sigma_p+\Sigma_s} \, du = \sum_i \frac{\Sigma_{ai} \Sigma_p \Delta u_i}{\Sigma_p+\Sigma_{al}}$$

Thus for each broad group we can obtain sets of Δu_{ig} which fit the results over the desired range of Σp. It is found in practice that 5 such sub-groups are adequate for Uranium-238.

In this representation it is necessary to obtain P(f→f) for each fuel cross-section in turn in order to evaluate the resonance integral and flux. A further refinement is to use a full spatial flux solution for each sub-group including the effect of heavy cans, etc. This route is described by Roth (9). This method is capable of estimating cross-sections for sub-regions within the fuel to any degree of refinement for which an appropriate flux solution can be obtained for the sub-group. A simple application is to determine the spatial build up of Plutonium within a pin, shown compared to experiment in Figure 4. The method can also be used to determine cross-pin effects. In its simple form it is limited, as is the equivalence method, to treating fuel of uniform temperature, and recourse is had to earlier results (10) to justify the use of mean fuel temperature in such calculations.

3.5 RESONANCE OVERLAP

The overlapping of resonances has been referred to earlier. The effect of Uranium-238 resonances on Uranium-235 and Plutonium-239 fission was dramatically illustrated in an experiment by Sanders (11) in which a fission chamber was moved through a central hole in Cadmium covered rod of Uranium-copper-Uranium. Figures 5 to 7 show the rise of fission rate when the fissile material was not shielded by Uranium-238.

It can be shown that the effect is primarily one of reduced neutron flux in the resonances, and so long as this is correctly allowed for in the calculational method the major part of the effect will be modelled. A smaller effect of Uranium-235 on Uranium-238 can be shown theoretically to be of the order of 1% enrichment. It is, however, just sufficiently important to require modelling. A simple representation is used in the WIMS code (1).

3.6 GROUP REMOVAL DATA

The group removal cross-sections in the resonance region will be sensitive to the amount of resonance absorption. In a few-group model some correction must be made for this effect.

The effect may be seen in its extreme form by comparing the group form of solution with the analytic one for a homogeneous medium and relatively heavy scatterer which does not slow down more than one group.

$$p = \exp - \frac{I}{\xi\Sigma s} = \frac{\Sigma_R}{\Sigma_R + \Sigma_A}$$

Now in the absence of absorption,

$$\Sigma_R = \xi\Sigma s / [\Delta u - I/\Sigma s]$$

whilst we have determined that

$$\Sigma_A = I / [\Delta u - I/\Sigma s]$$

we require

$$\frac{\Sigma_R'}{\Sigma_R' + \Sigma_A} = \exp - \frac{I}{\xi\Sigma s}$$

if we write $\Sigma_R' = \Sigma_R . f(p)$ we obtain

$$\frac{\xi\Sigma s . f(p)}{\xi\Sigma s . f(p) + I} = 1 - \frac{I}{\xi\Sigma s} + \frac{1}{2!} \left(\frac{1}{\xi\Sigma s}\right)^2$$

$$= 1 - \frac{I}{\xi\Sigma s . f(p)} + \left(\frac{I}{\xi\Sigma s . f(p)}\right)^2$$

$$f(p) \simeq \frac{2p}{1+p}$$

The correction is normally small for heterogeneous systems except in the intermediate spectrum range. Alternative models are possible, corresponding to higher order integration over lethargy. One such model is to retain the group representation but to introduce non-physical transfers from higher energy groups so that the escape probability is maintained regardless of the within group absoption.

3.7 VALIDATION

By careful choice of models, and relating the solutions to the most relevant situations which can be exactly modelled, it is possible to minimize errors introduced, for example in the treatment of resonance scattering. It is difficult to quantify the residual model uncertainties, however, and it is highly desirable that the eventual model be compared to Monte Carlo solutions - using an identical data base - for a number of cases in the range of practical interest. In the case of the models

used in the WIMS code it was found that even when oxide and metal fuels were represented by the same set of tabular data a few-group equivalence model could be relied upon to introduce errors of less than 1% in resonance capture for a wide range of problems. Typical comparisons are shown in figure 3.

4. DISCRETE ORDINATE METHODS

4.1 BASIC FORM OF THE EQUATION

Having simplified the original problem into a few (~100) group form we have a choice of methods by which to obtain the desired space/energy/angle solution. The simplest integral transport formulations have been reviewed briefly. The most common alternative is the discrete ordinate method, a differential technique.

In slab geometry, the version of the method due to Carlson is simply described. The angular flux within a group determined along lines at discrete angles θ_i with the normal to the slab surfaces. The transport equation may be simplified within each spatial region of constant material composition to be:-

$$\mu_i \frac{dN_i}{dx} + \Sigma_t N = S = \sum_{g'} \Sigma(g' \to g) \phi_{g'}$$

where $\mu_i = \cos \theta_i$

$N = N(X, \mu_i)$ is the angular flux

Σ_t = total cross-section

$\Sigma(g' \to g)$ = Inter-group transfer (all processes)

$\phi_{g'}$ = scalar flux in group g' $= \frac{1}{n} \sum_i N(\mu_i)$

If the source term S is taken to be constant over a mesh interval Δ it will be seen that the equation can be integrated over the mesh to give

$$N(x) = N_o \exp\left(-\frac{\Sigma_t x}{\mu}\right) + \frac{S}{\Sigma_t}\left[1 - \exp\left(\frac{\Sigma_t x}{\mu}\right)\right]$$

and the mean angular flux $\bar{N}$ can be deduced from neutron balance to satisfy

$$\text{Collisions} = \bar{N} \Sigma_t \Delta = (N_o - N_1)\mu + S\Delta$$

where N_o N_1 are fluxes entering and leaving the mesh interval. Carlson uses the rational approximation

$$\exp\left(-\frac{\Sigma_t \Delta}{\mu}\right) \quad \frac{1 - \frac{\Sigma_t \Delta}{2\mu}}{1 + \frac{\Sigma_t \Delta}{2\mu}}$$

to give

$$N_1 = \frac{N_o\left(1 - \frac{\Sigma_t \Delta}{2\mu}\right) + S\Delta}{1 + \frac{\Sigma_t \Delta}{2\mu}}$$

to provide a particularly simple set of equations. It has often been surprising that these equations gave good results outside the apparent limits of validity of the derivation; indeed for course meshes it could be better than the exact solution for constant source in the mesh. The reason for this can be illustrated simply in a one-group form with fixed source Q by writing

$$\mu \frac{dN}{dx} + \Sigma_t N = Q + \Sigma_s \phi$$

$$\mu \frac{dN}{dx} + \Sigma_a N = Q + \Sigma_s(\phi - N)$$

It will be seen that the usual integration assumes ϕ constant over the mesh. Suppose instead that we assume $(\phi - N)$ constant. This parallels the usual approximation of diffusion theory because $\phi - N$ is proportional to neutron current in diffusion like situations.

The previous derivation is modified to give

$$N_1 = N_o \exp\left(-\frac{\Sigma a \Delta}{\mu}\right) + \frac{Q + \Sigma s\ (\bar{\phi} - \bar{N})}{\Sigma a}\left(1 - \exp\left(-\frac{\Sigma a \Delta}{\mu}\right)\right)$$

$$\bar{N} \Sigma_a \Delta = (N_o - N_1)\mu + \left[Q + \Sigma_s\ (\bar{\phi} - \bar{N})\right] \Delta$$

Interestingly, if we make the same rational approximation as before, but for exp $-\frac{\Sigma a \Delta}{\mu}$, we find that the same equations are obtained as in our original derivation. Thus $\frac{\Sigma t \Delta}{\mu} << 2$ is a sufficient, but not necessary condition for Carlson equations to hold.

4.2 TREATMENT OF CYLINDRICAL GEOMETRY

The standard route for generalization of the discrete equations to cylindrical geometry follows earlier spherical harmonics practice. The term in $\frac{dN}{d\mu}$ has now to be modelled, and the equations, making the same assumptions as before, have the form

$$\eta_j \mu_{ji} (\bar{N}_{jir} - \bar{N}_{jir-1}) + \eta_j b_{ji} \frac{\Delta r}{2\bar{r}} (\bar{N}_{jir} - \bar{N}_{jir-1}) - \eta_j b_{ji} \frac{\Delta r}{2\bar{r}}$$

$$(N_{j\,i-1\,r} + \bar{N}_{j\,i-1\,r-1}) + \frac{\Sigma t \Delta r}{2} (\bar{N}_{j\,i\,r} + \bar{N}_{jir-1}) = r \Delta r \bar{S} \text{ with}$$

$$N_{ji} = 2\bar{N}_{ji} - N_{j1-1};\ b_{ji} - b_{ji-1} = -(\mu_{ji} + \mu_{ji-1})$$

to integrate these it is necessary to start with the equation $\mu = +1$ which does not require a backward difference in μ to solve, and then to step in $\Delta\mu$. Examination of the procedure shows that the choice of constant set of μ_i corresponds to solutions along equiangular spirals as shown in the right hand side of Figure 8. The terms in $\frac{dN}{d\mu}$ clearly arise because the track leaving a spatial mesh region is in a different direction from that entering it.

An alternative formulation is to track neutrons along straight-line paths as shown on the left of the Figure. The equations to be solved along each line are then the same as those in slab geometry, the characteristic form of the equation (14). The integrating mesh is then the same as that used in numerical estimation of collision probabilities.

4.3 BOUNDARY CONDITIONS

In order to reduce an infinite lattice problem to a cylindricalized form, some approximate treatment of the boundary is required. It is usual to define the outer cylindrical boundary in such a way as to pressure the volume of unit square of hexagon (although there are some exceptions to this which are discussed in a later section). Three major options are available.

(a) Specular Reflection. In this case neutrons are perfectly reflected as the cylindrical boundary of the model. This model tends to error as the dimensions of the unit cell become small because the chord-lengths distribution is grossly disturbed. As pointed out by Newmarch, paths missing the fuel on one cell crossing never intersect fuel, whilst those passing through the fuel do so on every crossing.

(b) Isotropic Return at Each Altitude. In a discrete ordinate calculation separate estimates of angular flux are available at different angles to the pole. Outgoing neutrons are returned isotropicaaly in such a manner as to presume neutron balance separately at each such angle. This retains one element of realism in the model for cases in which the long paths in the outer region at anles near the pole are important, but removes the correlation inherent in specular reflection. This was called a white boundary condition when first introduced.

(c) Isotropic Return Over all Angles. This is the condition most easily used in collision probability formalism, because reciprocity relations exist to determine the probabilities of incoming neutrons with such a distribution colliding in each region in terms of the corresponding outgoing probabilities. It can also be simulated by introducing dummy scattering zones outside the true boundary. For most cases this condition gives results close the those of the previous case, but it is less good and should be avoided if possible.

In the case of characteristic formulations, better approximations to the true boundary can be obtained by avoidind explicit cylindricalization. Consider a case in which a square boundary is retained, and the same number of tracking lines is used as in the cylindrical model of Figure 8. We may, as an alternative, use these in two families inclined to each other at 45° and having boundary conditions determined correctly on physical grounds. This option is a new one and is currently being studied.

4.4 CHOICE OF INTEGRAL OR DIFFERENTIAL METHOD

Both solution techniques should be capable of giving the same answer if a sufficiently high order of representation is used, with the exception of the limitation boundary condition for the integral method. This will only be significant for very close packed systems. The solution techniques used in the innermost loop may be contrasted on the assumption that the outer iteractive strategy is the same in both cases. For the integral method

$$\underline{\Psi} = P\,\underline{\Psi}$$

where Ψ is scalar flux reactor over space

Ψ is emission density reactor over space

P is (full) collision probability matrix

Whilst for the differential method

$$N_{i,j} = a\, N_{i-1,j} + b\, \Psi_{ij}$$

$$\phi_i = \frac{1}{n} \sum_j N_{i,j}$$

Thus for m space regions the former requires a number of operations proportional to m^2 whilst the latter is proportional to nm,n being the number of angles required. We may deduce that the differential method will be less expensive for problems involving a large number of meshes, and a specific illustration of this (using the two codes WDSN and PERSEUS) is shown in Figure 16. The relation normalization of the two methods will, of course, depend upon efficiency of coding etc, but the basic behaviour is clearly tending to the expected asymptote. In this case the break even point was less than 10 regions.

5. THE TREATMENT OF LEAKAGE

5.1 INTRODUCTION

Our presentation so far has been concerned with the solution of infinite arrays of identical rods, and some more or less arbitary eigenvalue has been introduced to permit solution of the equations. In real systems, neutrons pass from cell to cell and may ultimately leak from the system. The case of all uniform lattice is a special one, and may simply be illustrated by considering an array of fuel pins of negligible size (line sources and sinks) finite in one dimension x. Suppose that a neutron born in fission in a pin at x_i has a probability of causing fissions at x_j

$$k_{ij} = k\,(|\, x_i - x_j |\,)$$

Suppose that there is a solution $f_i = f(x_i)$ which is critical, then

$$\sum_i k_{ij} f_i = f_j \qquad \text{for all } j$$

as k_{ij} is symmetric this clearly implies a condition on curvature, and there will be solutions of the form

$$f_i = Ae^{iBx}$$

where B may be real or imaginary. The solution thus has a real curvature B^2 the critical buckling. Consider a pin at $x_o = 0$. Then for a regularly spaced lattice we have a critical condition

$$K_o + 2K_1 \cos B\Delta + 2K_2 \cos 2B\Delta + \ldots = 1$$

Now our infinite lattice multiplication

$$K = K_o + 2K_1 + 2K_1 + \ldots$$

hence $K_\infty - 1 = 2K_1 (1 - \cos B\Delta) + 2K_2 (1 - \cos 2B\Delta) + \ldots$

$$\text{expanding} = B^2 \Delta^2 \left\{ K_1 + 4K_2 + 9K_3 + \ldots \right\} - \frac{B^4 \Delta^4}{12} \left\{ K_1 + 16K_2 + 81K_3 + \right\} + \ldots$$

$$= \frac{B^2 \bar{X}^2}{2} - \frac{B^4 \bar{X}^4}{24} + \ldots$$

where $\bar{X}^2$ is the mean square distance travelled in one generation from fission to fission. In the limit as $\Delta \to 0$ we obtained an homogeneous result. Note that no constraints have been placed upon the energy/angle form of the solution at this stage.

5.2 HOMOGENEOUS MODELS

Homogenization of the model problems is practical so long as at least the lower powers of $\bar{X}^{2n}$ are preserved in the process. If we wish to homogenize in a way that conserves all events in our multi-group model - including group-to-group transfer, there is only one free parameter available to fit this - Σgg in transport theory or the diffusion coefficient Dg in diffusion theory. This can in principle be done exactly in the special case of a buckling mode.

The basis of this method is treated in standard texts. One particular restriction may be noted when diffusion theory is used in the final modelling stage. This imposes restrictions on the possible form of the kernel

$$k = A_e^{-\kappa|x_i - x_j|} \qquad \text{When } \kappa = \sqrt{\Sigma a / D}$$

hence

$$\bar{X}2 = \int_0^\infty x^2 e^{-\kappa x} dx \Big/ \int_0^\infty e^{-\kappa x} dx = 2/\kappa 2$$

$$\bar{X}4 = \int_0^\infty x^4 e^{-\kappa x} dx \Big/ \int_0^\infty e^{-\kappa x} dx = 24/\kappa 2$$

$$\text{Hence } 1 = \frac{k\infty}{1 + B^2 M^2} \qquad M^2 = D/\Sigma a$$

Age theory similarly serves to preserve the second moment.

5.3 TREATMENT OF VOIDS

The effect of cross-section differences in the medium, of which voids are the extreme case, is traditionally described as 'streaming'. In extreme cases it can be shown that no asymptotic solution of a buckling form may exist, although in practice quasi-asymptotic solutions are observed. (An example is a semi-infinite slab system with cylindrical holes normal to the surfaces).

Exact solutions may be obtained for such problems using either differential or integral formalism. Monte Carlo methods lend themselves to direct determination of the transport kernal, from which we may deduce either the successive moments needed for leakage calculation, or, more simply, determine the ratio of multiplication with and without leakage. For, in the simplest case, suppose that a neutron standard at x = 0 yields or neutrons at x. By symmetry, the converse will apply in a cylindrical lattice. Thus the sample may be considered to contribute

n_i to the estimate of k-infinity

$n_i \cos BX$ to the estimate of k-effective

$k\infty = \langle n_i \rangle$

$keff = \langle n_i \cos BX_i \rangle$

The differential formalism, for example in discrete ordinate methods, involves a weighting of the angular fluxes. This can easily be seen, for example in a one-dimensional geometry with leakage in a transverse direction.

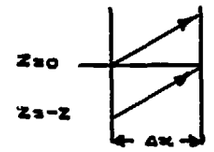

The neutron leaving one face at z = 0 may be considered to be 'replaced' at the second face by that from -z. Then the flux is reduced by cos Bz = cos B Δ X/μ compared to that in the non leakage application. The method has been successfully used in cylindrical geometry, but demands a higher order angular quadrature in the direction of the leakage than would normally be used.

5.4 SIMPLIFIED MODELS

A number of simple prescriptions are available for treating particular types of streaming problem. The most commonly used are those due to Behrens (for a range of hole geometries in an otherwise uniform medium) and Benoist (usually used in its simpler form for a 3-region lattice of fuel, void, moderator).

5.5 RESTRICTIONS OF APPLIABILITY

Equilibrium leakage models, dependent upon the existence of zones of asymptotic leakage properties, are useful models for many simple experimental applications. Because flux curvature is the same in all groups they relate the leakage to a particular energy-dependence. It is not necessary to apportion 'leakage' exactly over energy, and a diagonalized (diffusion-like) model is acceptable. Heterogeneous lattice problems are not necessarily solved using the same approximation.

6. TREATMENT OF ASSEMBLY GEOMETRY - EXACT

6.1 INTRODUCTION

As the most common types of reactor exhibit a double heterogeneity of pins in assemblies a fully explicit spatial solutions is difficult. In practice the only route which has been exploited for this purpose is the collison probability one, usually with some restriction, for example to isotopic scattering models.

The two major deterministic code options relating to cluster and box geometries are described briefly below. It is interesting to note that differential methods, despite the advantages to be expected in many region problems, have not been seriously exploited, although one case has been reported in which

the method of characteristics was applied to a simple BWR benchmark problem.

It is usual to apply some form of condensation in energy before using methods of this kind so as to reduce the labour of solution.

6.2 PIJ

Axially uniform, the code allows a basic r,θ geometry upon which can be superimposed rather general distributions of cylindrical rods, themselves subdivided in r and θ. The θ mesh may vary with r (mesh deletion) and periodicity in θ can be allowed to reduce the number of regions solved.

The outer boundary may be determined by surfaces within this co-ordinate system, as in the HTR case illustrated in Figure 9 or may be square, an option convenient for pressure tube reactors and the Advanced Gas-Cooled reactor. Rods at the boundary are permitted so long as they as symmetrically placed; for example interstitial rods are modelled.

6.3 CLUP

In the x-y plane a cartesian mesh is imposed. Within each mesh a single nest of cylinders subdivided in radius may be specified. The associated 'coolant' may be divided into quadrants. The geometry is that of PWR or BWR lattices, albeit with limited possibilities of sub-division.

6.4 MONTE CARLO METHODS

Monte Carlo methods are most commonly used in solutions of problems where a single parameter such as the multiplication of an assembly is required. This reflects the underlying statistical properties of estimation inherent in the method. For the simplest tracking procedure consider an event having a probability p. The standard deviation on the estimation of this is

$$\pm\sqrt{\frac{p(1-p)}{n}}$$

where n is the number of neutrons tracked. It will be seen that the determination of rating, say, in a particular pin of a 17 x 17 assembly will require a large sample and correspondingly high using such a direct method.

The technique does, however, permit simple codes to be written to deal with the most complicated geometries, and to model nuclear processes such as anisotropic scatter or resonance capture to any desired degree. There are, as a consequence, certain types of calculation for which they are preferred.

A fairly new application is their use in determining neutron migration in infinite systems to model leakage, especially in complicated geometries.

For successful power distribution studies it is likely that some additional smoothing technique would be needed. One option is to solve for the difference between the actual geometry and an homogeneous one of similar average properties. In this way the Monte Carlo would be sampling only for smaller quantities (pin to pin difference in rating) which might be x 10 smaller than the rating itself. In this case comparable accuracy could be achieved with x 100 less neutrons tracked. The method has been applied to a few special problems but not widely exploited.

7. TREATMENT OF ASSEMBLY GEOMETRY - APPROXIMATE

7.1 THE PROBLEM

If the pins and their surrounding coolant can be smeared into a single effective material the geometry usually reduces to a simpler form which can be solved using less elaborate codes. In the case of cluster geometries a cylindrical approximation is often adequate for the reduced geometry, whilst for LWR assemblies an x-y transport (or even diffusion) model will be needed. As in the leakage treatment the only free parameters after all within group reaction rates are preserved will be the diffusion coefficient or transport cross-section and this precludes an exact solution.

7.2 THE PROCOL METHOD

Although more applicable to grain in annulus geometry, and used mainly for HTR and burnable poison calculations, the approximation in PROCOL illustrates the most developed approach. In this, for each of the smallest units of geometry, say a spherical grain, the collision probabilities are calculated, including the probability of escaping to the boundary. By reciprocity, the probability of neutrons isotropically incident upon the sphere crossing it and escaping can be calculated.

$$P(S\to S) = 1 - \sum_j P(S\to j)$$

$$= 1 - 4/S \sum_j \Sigma_j V_j P(j\to s)$$

The grain may then be replaced by an homogeneous one having the same transmission probability by choice of an appropriate total cross-section. Within the limitation of the isotropic boundary flux approximation, probabilities of transferring between

all homogeneous regions may be calculated. As the total collisions in the smeared region or regions have been preserved, it is possible to symthesize all the collision probabilities in the original problem. For example if j is a sub-region of J we may compute

$$P(I \to j) = P(I \to J) \frac{P(S \to j)}{\sum_1 P(S \to i)}$$

and similarly for all other collision probabilities.

7.3 FLUX SMEARING

The same problem may be posed in differential form. For consider a straight-line track crossing the region to be homogenized. The collisons within the zone lead to removal of neutrons from the beam, and in the absence of sources we obtain

$$N_{out} = N_{in} e^{-\bar{\Sigma}\bar{L}}$$

where

$$\bar{\Sigma}\bar{L} = \int_{region} \Sigma_t (x)\, dx$$

It is easily seen that this component along each line is reproduced by the volume average cross-section along the line. To produce the total transmission probability over the zone requires that for each direction of incoming flux, N,

$$\text{Current out} = \int_{region} N_{in} (y)\, e^{-\bar{\Sigma}\bar{L}(y)}\, dy$$

The series/parallel element in matching this solution, even for known $N_{in}(y)$ is seen to present a severe problem. The presence of sources Q in the region gives another component of outgoing flux

$$\int \frac{Q(x)}{\Sigma(x)} (1 - e^{-\bar{\Sigma}\bar{x}})\, dx$$

$$\bar{\Sigma}\bar{x} = \int_{x}^{boundary} \Sigma_t(x)\, dx$$

It will be seen that reduction of the equations to an homogeneous form requires a number of approximations which will best be made allowing for the characteristics of the problem to be solved. For example in a gas-cooled or voided lattice the neutron sources over most of the energy range will be negligible, but the total cross-section will be very different between fuel and coolant. At the opposite extreme, for a water filled lattice, the transport cross-section will not vary markedly between materials but the correct treatment of source will present a problem.

The most commonly used approximation is to weight all cross-sections with an estimate of scalar flux obtained by some subsidiary calculation. This preserves the relative reaction rates, for example in fuel and coolant, but will not be a particularly good approximation for the transmission across the region except in the limit as the heterogeneity tends to zero (either uniform cross-sections or many small sub-regions uniformly distributed). In other cases, the model must be justified against more exact methods.

7.4 SOLUTION IN SMEARED GEOMETRY: AIMS OF HOMOGENIZATION

In pressure tube reactor designs it is often sufficient to solve the resultant problem using transport models in cylindrical geometry. For water reactors the flux variations within the box are generally smaller, at least in the absence of control absorbers, and the use of x-y diffusion theory is considered adequate. Special problems arise if we wish to use x-y transport theory in its usual form, the diamond difference scheme due to Carlson and used in codes such as TWOTRAN. Lack of detailed angular neutron balance in the formulation leads to ray effects which can distort the flux solution. The problem is not usually numerically important in single reflective assemblies compared to the uncertainty introduced by homogenization, but may become more significant if whole reactors are modelled. The effect can be illustrated simply for a special case of a square mesh in which we consider only neutrons travelling at 45° to the mesh lines

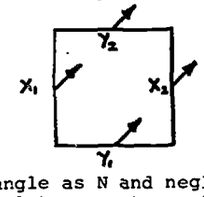

denoting the flux in this angle as N and neglecting sources for simplicity, we have the usual transport equation in the plane

$$\mu \frac{\partial N}{\partial x} + \sqrt{1-\mu^2}\, \frac{\partial N}{\partial y} + \Sigma_t N = 0$$

For our special case $\mu = \sqrt{0.5}$ and we write

$$\frac{1}{N2}\left(\frac{X_2-X_1}{\Delta X}\right) + \frac{1}{\sqrt{2}}\left(\frac{Y_2-Y_1}{\Delta Y}\right) + \frac{\Sigma_t}{4}\left(X_1+X_2+Y_1+Y_2\right) = 0$$

Given incoming solution X_1, Y_1 from previously solved meshes we see that this equation is not sufficient to determine X_2, Y_2. A further condition is imposed depending upon smoothness of the angular flux

$$\frac{X_1+X_2}{2} = \frac{Y_1+Y_2}{2}$$

which yields the desired solution. The problem arises because the angular flux is generally not smooth in the direction perpendicular to the direction of neutron motion. Changes in cross-section at material boundaries lead to singularities in slope in this direction. In our special case we can solve exactly

$$X_2 = Y_1 \exp\left(-\frac{\Sigma_t \Delta x}{\sqrt{2}}\right) \qquad \text{etc}$$

It will easily be seen that if the incoming fluxes X_1, Y_1 differ significantly - for example if one of them were adjacent to a black cruciform absorber $Y_1 = 0$, we obtain for our simple problem

Diamond Difference	Direct Solution
$Y_2 = \dfrac{X_1}{1 + \Sigma\Delta/2\sqrt{2}}$	$Y_2 = \dfrac{X_1\left(1 - \Sigma_t\Delta/2\sqrt{2}\right)}{1 + \Sigma_t\Delta/2\sqrt{2}}$
$X_2 = -\dfrac{X_1\,\Sigma\Delta/2\sqrt{2}}{1 + \Sigma\Delta/2\sqrt{2}}$	$X_2 = 0$

Thus although a similar neutron balance is obtained, neutrons are shifted in position as a result of the approximation. It is easily seen that the effect is not removed as the mesh size is reduced. Great care is therefore required in the use of codes of this type for just the class of problems for which diffusion theory is likely to prove inadequate.

7.5 USE OF MODIFIED DIFFUSION COEFFICIENTS

Even for problems in which the conditions for direct derivation of the diffusion equations do not hold, correct solutions may be obtained by the appropriate choice of diffusion coefficient. In one dimension it is always possible to match diffusion and transport solutions exactly by direct substitution in Ficks Law once the answer is known. Although exact generalization to two or more dimensions is not possible, it is often valuable to introduce a modification to the diffusion coefficient based upon a simpler solution. A good example is the treatment of cruciform control absorbers where constants deduced from one dimensional studies may be introduced into a two dimensional solution (especially one in which the diffusion coefficient is allowed to be differed in x and y directions. Near black boundaries the transport solution exhibits greater flux slope than the diffusion one, and the general effect is to reduce D below the value appropriable far from boundaries. A similar effect is obtained by the substitution of double-Po theory for diffusion theory as being more appropriate near discontinuities in cross-section. In this case we obtain

$$D(\text{double Po}) = {}^1/_4\,\Sigma t \qquad D(\text{diffusion}) = {}^1/_3\,\Sigma t$$

As in cell calculations there is less interest in solution far from boundaries, it is not unreasonable to use this approximation throughout in the absence of better models.

7.6 USE OF MULTI-CELL COLLISION PROBABILITIES

One alternative to homogenization in the approximate treatment of complicated geometries is the multi-cell method. Logically similar to the synthetic collision probability method previously considered, its development started from a different type of problem. In many cases in which the problem may be seen as an aggregate of simpler geometries the boundary conditions linking the regions are simply defined. This is normally linked with the situation in which transmission across the sub-units is small. In such cases a collision probability matrix can be synthesized without recourse to an explicit solution in the homogenized (highest level) geometry.

The first application of the method was to chequerboard geometries. In this case all neutrons leaving a 'black' cell clearly enter a 'white' one and a simple generalization of the usual reflective boundaries condition is possible so long as the nett current between cells is sufficiently small to be treated as isotropic in the cylindrical approximation.

The method has since been generalized to treat a wide range of geometries. Two problems are highlighted in such applications.

1. Transmission across cells without collision. It is usually simple to define the probability that a neutron leaving a particular cell will enter each of a number of other cells, but the synthetic collision probability route needs to determine the probability of colliding in it. As geometry units become smaller this fraction becomes more important and some approximation must be made to deal with it. The simplest route is to estimate the transmission probability for the region and to apportion the transmitted neutrons rather arbitarily in the same way as the total neutrons leaving the cell-type. Thus for two types, if the probabilities of leaving type A entering type A or B is P_{AA} P_{AB} etc, we can determine the probability R_{AB} or colliding in type B as follows, if we write x as the transmission probability of neutrons entering B and y that of neutrons entering A

$$R_{AB} = (1-x)\ P_{AB} + x\,P_{AB}\ P_{BA}\ Y\,P_{AB}(1-x)$$

$$+ x\,P_{AB}\ P_{BB}\ (1-x)\,P_{AB}$$

$$= (1-x)\,P_{AB} \quad 1 + (1-x)\,x\,P_{AB} \quad \left[y\ P_{BA} + P_{BB}\right] + ..$$

more tractable is the form

$$R_{AB} = (1-x)\ P_{AB} + x\,P_{AB}\ R_{BB}$$

which leads to a matrix equation for $\underline{R}$ in terms of $\underline{P}$ x and y. Note that $\underline{R}$ is now group dependent.

2. Different Cell Surface Areas

Implied in the geometric determination of the matrix of probabilities P is that the surface of a cell is contiguous with a similar surface of other cells. This self-evident property may be lost after cylindricalization - for example if the lattice is divided into octagons and squares. In this case the reciprocal relationship is violated and significant errors in cell-to-cell flux arise. The simplest option is to choose a cylindricalized model preserving cell surface area as well as conserving material; this implies a reduction in density of the outermost zones of the cylindrical model. It is intuitively satisfactory to change the density only outside the inscribed circle of the true geometry, but within the errors of approximation little difference has been found between different models.

Errors in the space/angle assumptions made in deriving the multi-cell equations lead to errors in determining inter-cell current and thus relative fluxes or powers in the cells. They can often be minimized by suitable choices of boundary aimed at placing these in positions of minimum gradient or current. For example if a chequerbaord contained alternate strong and weak absorbers it would be helpful if a larger cell volume were associated with the former. Some additional model refinements, akin to course mesh corrections, are possible to deal with tilts in simple geometries.

Because of the problem of accurate determination of boundary conditions, multi-cell models are usually avoided for determination of relative absorptions or powers where high accuracy is needed. Good examples of their use are:-

1. Treatment of assemblies at the fine-group stage so as to give a representation of the interaction between regions in determining condensation spectra.

2. Treatment of detailed sub-geometries in repeated calculations, such as spatial depletion of burnable poisons, where absolute normalization can be established by exact calculations at least for the initial configuration.

The method has, however, been found to be of value in practical problems, such as treating driver assemblies in reactor experiments, where the geometry may be so complicated that no better model can be used.

8. MODELLING OF DEPLETION

Having obtained an adequate space-energy description of events in the lattice cell it will be necessary to relate this to events in the reactor in which depletion and various forms of control operation are of significance. The modelling of this will be simplified in some way and the information from the cell calculation needs to be passed to it in a usable form. We discuss here the most common these, homogenized cell data, but exactly similar considerations apply where heterogeneous models are used.

Depletion in the whole reactor geometry may be treated at different levels. The most significant distinction lies in the degree of representation of the isotopic composition of the fuel. At one extreme this may be determined from the lattice calculation, in which case only microscopic (smeared) cross-sections as a function of irradiation need to be supplied to the main calculation. Such models mean that the environment has to be represented in some way during the cell burnup if high accuracy is to be achieved, especially in circumstances in which it would effect the conversion ratio. Thus different sets of data for the same cell could be needed, for example depending upon proximity to the reflector.

In particular, because a large part of the capture in Uranium-238 occurs at resonance energies, the balance between these and thermal flux is most important. In a light water moderated reactor most transfer of neutrons between assemblies takes place at high energies and the method used to model it is of little importance. For graphite and heavy water moderated systems it is important to maintain the cell critical by simulating its environment in some simple way, such as variation of a component of buckling, etc.

It is clear that when the composition of the lattice cell is fixed in this way as a function of irradiation the benefits of detailed energy solutions in the whole reactor environment must be relatively small, and it is uncommon to see such a route implemented in more than two energy groups.

The next highest degree of representation involves the explicit representation of some number of nuclides in the whole reactor calculation. The lattice cell or assembly calculation can then be less well represented, especially so far as environment is concerned, because it will be a source only of few-group cross-sections for such nuclides. Models of this kind may be used for various levels of representation:-

1. For soluble poisons or other control options which are essentially instantaneous changes.

2. For power dependent components, primarily Xenon.

3. For a small number of key quantities related to conversion ratio - perhaps ^{238}U ^{235}U ^{239}Pu.

4. For most burnable species, simplifying only fission products or other slowly varying components.

Even at this degree of representation the constants will represent significant condensation over space and energy, and will thus be problem dependent. This is especially true for high cross-section materials reaching some sort of saturation (for example ^{240}Pu) in which it is easier to determine the macroscopic cross-section $\Sigma = n\sigma$ than either number density or microscopic cross-section. For this reason it may be essential to make the microscopic cross-section tabulations have a specified dependence upon concentration, the equivalence of a shielding law for resonances. Thus the cross-section might be assumed to be of the form

$$\sigma = \frac{\sigma_o}{1 + c\sqrt{n}}$$

and an appropriate interpolation procedure can then be devised to obtain an appropriate cross-section between tabular points, say at two different irradiations.

In all such cases the representation of changing water density poses the most difficult problems.

9. BOUNDARY CONDITION PROBLEMS

9.1 INTRODUCTION

Most established calculational methods rely upon the production of homogenized pin or assembly data and its subsequent use in whole reactor calculations based upon diffusion theory. Newer approaches are, however, under development and we explore the basis of some of these.

The key question in all such approaches is to dientify an approximately simplified boundary condition at an assembly interface. We consider a small number of possible ways in which this might be done.

9.2 THE SNAPSHOT MODEL

Is particularly appropriate in situations in which a single assembly has some unusual feature requiring special modelling methods. A particularly simple case was the one illustrated in Figure 22 in which the central block of an HTR experimental assembly had two non-symmetrically placed control rods, generating a tilt across it, and across the otherwise uniform reactor.

In this case an appropriate set of boundary conditions were sought to model the remainder of the reactor at the surface indicated in the Figure. It is clear that if at any non-re-entrant boundary in the reactor we can establish for a neutron crossing in one direction the space/angle/energy probability of returning in the opposite direction then we can separately solve the two parts of the total system. Suitable choice of boundary - preferably in a large moderating region - may allow us to obtain adequate results using a simplified boundary condition.

For the particular problem at issue the symmetry of the reactor outside the central block was a key issue, for this ensured symmetry in the boundary condition. The near homogeneity of the reactor as a whole, and absence of heavy absorbers, suggested that diffusion theory would be an adequate model. Then solution of the whole reactor problem on a triangular mesh with a number of arbitrary assymetric changes within the boundary was interpreted in terms of gross ingoing and outgoing fluxes and currents to give the appropriate boundary condition.

The technique can be applied at two levels:-

1. A within-group boundary condition in which all returned neutrons are redistributed only in space. This depends for its success upon a good basic solution to the overall problem.

2. A full space-energy return condition. This is more labourous to construct and to use, but will be less sensitive to the model used in generating it. Because of the important effect of fission in determining effective returns from a distance the form of the condition will tend to be a localized space-energy return characteristic of return after few collisions, plus a smoother, space/energy return, independent of the outgoing neutron energy except in its normalization.

Even the first of these models proved very effective for the particular problem studied, and led to a good representation of across-cell tilts.

9.3 ASSEMBLY AND ASSEMBLY SOLUTIONS

The inverse problem is posed in terms of replacing a fuel assembly by a mechanism transferring neutrons to its boundaries. The reactor as a whole can then be modelled by connecting all the assembly solutions. The same problems arise as in the snapshot solution.

1. What degree of refinement is space/angle/ enrgy is needed at the boundary to characterize the solution.

2. Should the transfer mechanism be a full space/angle/energy one or should it be truncated to some effective form (for example to a within group representation).

Both types of model have been considered. We offer here some general comments which may help to clarify the issues involved.

Firstly, on physical grounds, we can easily see that the great majority of neutrons leaving an assembly having entered at its boundary will have undergone one or more fissions. This is especially true for all boundaries other than that of entry. Thus it is to be expected that the outgoing neutrons will be largely decoupled in energy from the incoming ones. It would be perverse, in this case, to attempt to diagonalize the operator in energy.

Secondly, because only the total probability of emergence is significantly affected by the energy or angle of entry, it should not be necessary to operate the whole reactor calculation in many energy divisions.

In developing a scheme of this kind it is clear that consideration should be given to overlapping group or eigenvector expansion models as possible ways of limiting the number of energy variables.

This class of methods may be related to conventional coarse mesh models for whole reactor geometries for the special case in which few-group diffusion theory is an adequate model. It is interesting and important to note that spatial condensation of the diffusion equations over an assembly does not in turn lead to a diffusion-like finite difference form except in the spatial case of one group.

9.4 KERNEL METHODS

For pressure-tube reactors, and similar heterogeneous core layouts, an alternative exploitation of this general type of model is possible. A generalization of the method of Feinberg and Galanin, it involves a finite lattice due to a fission source in one of the channels. In the (unpublished) examples studied, this kernel was computed by a Monte Carlo simulation in group form, which may be regarded as a special case of lattice cell calculations.

Because the distribution of absorptions in the nearly black fuel channels is not sensitive to small changes in absorption cross-section, it is possible to use the same kernel for a range of situations. More precisely, for the case of fuel differing only in enrichment in burnup, there are significant differences in the distribution of events only at thermal energies. Suppose that we have available the kernel for the highest cross-section in the core. Then lower cross-sections may be modelled by restarting an appropriate fraction of neutrons and 'tracking' them again with a different thermal kernel. Thus total transfers between two channels i and j may be written

$$A\ (i \to j) = K(i \to j) + \sum_k K(i \to k)\ \frac{\Delta\Sigma_k}{\Sigma_k}\ T(k \to j)$$

It will readily be seen that because the fuel geometry is explicitly represented, and thus the 'restarted' neutrons contributing to the thermal kernel T(k→j) begin life within fuel pins, this kernel will be highly diagonal and may in many practical cases be neglected. The obvious exception arises in the treatment of reflectors.

9.5 SUMMARY

This group of methods, involving new ways of synthesizing the whole reactor solution from the results of simpler calculations, are at present under active development. They represent an attempt to make best use of the information present in the assembly solution and to some extent duplicated in whole reactor solutions of the usual kind. Whilst this potential differ for different reactor types it is the writers view that emphasis will shift towards more elaborate assembly calculations of this kind.

10. CONCLUDING COMMENTS

In a presentation of this kind, it is usual, and proper, to emphasize the most difficult problems in the field, and to describe the most advanced methods which have been devised in attempting to solve them.

By way of conclusion, it should equally be pointed out that reactors can be, and have been, successfully designed and built, and safely operated, using simpler modelling techniques. The key to this is the systematic validation of methods against experimental data - the topic of a comparison series of lectures.

Although the ability to predict reactor behaviour to high precision is of economic importance, the designer and operator need above all to know what uncertainty is associated with any advice given to them. If I may presume to offer advice to physicists from countries less experienced in the use of nuclear power, it is this: whatever choice of calculational methods is made, it is vital that the approximations involved in them are critically appraised, and the resulting uncertainties in prediction are fully understood. That way success lies.

11. REFERENCES AND SUGGESTED READING

Lattice Calculation Schemes

1. ASKEW, J. R., FAYERS, F. J., KEMSHELL, P. B. A general description of the lattice code WIMS. Jour. Brit. Nucl. Energy Soc 5 4 p.564, 1966.

2. FAYERS, F. J. et al. LWR-WIMS. A Modular code for the evaluation of LWR lattices. Pt 1 Description of methods. AEEW - R 785 (1972).

3. ASKEW, J. R. Modular coding systems for reactor calculations. EACRP-A-135 ENEA Newsletter 11 (1971).

4. ROTH, M. J. Manual for Winfrith modular codes. AEEW - M 1001 (1970).

Collision Probability Methods

5. ASKEW, J. R. Review of the status of collision probability methods. p 185 Numerical Reactor Calculations (IAEA 1972).

6. ANDERSON, D. W. The WIMS-E module W-PIJ. A two-dimensional collision probability code with genral boundary conditions.

7. TSUCHIHASHI, K. CLUP 77. A FORTRAN program of collision probabilities for square clustered assembly. JAERI - 1196 (1971).

Resonance Calculational Models (see also References 1 and 2)

8. ASKEW, J. R. The calculation of resonance captues in few-group approximations. AEEW - R 489 (1966).

9. ROTH, M. J. Resonance absorption in complicated geometries. AEEW - R 921.

10. BEYNON, T. D., GRANT, I. S. Resonance capture and Doppler coefficient in cylindrical uranium lattices. Nucl. Sci. Eng. 23 368 1965.

11. CARTER, D. H., SANDERS, J. E. Shielding of resonance reactions in Uranium-235 and Plutonium-239 by Uranium-238. Jour. Nucl. Energy 21 565 1967.

12. ASKEW, J. R. The current UK position on Uranium-238 resonance capture. (Seminar on ^{238}U resonance capture BNL-NCS-50451 p45 1975).

Discrete Ordinate Methods

13. HENRY, A. L. Nuclear Reactor Analysis. MIT Press 1975 (strongly recommended for general introductory material).

14. ASKEW, J. R. A Characteristics Formulation of the Neutron Transport Equation in Complicated Geometry. AEEW - M 1108 (1972).

15. LATHROP, K. D., BRINKLEY, F. W. Theory and use of the General Geometry TWOTRAN Program. LA 4432 (1970).

Calculation of Leakage

16. BENOIST, P. Formulation generale et calculpratique du coefficient de diffusion dans un reseau comportant des cavites. Rapport CEA - 1354 (1959).

17. BRISSENDEN, R. J., GREEN, C. The superposition of buckling models on to cell calculations and application in the computer code WDSN. AEEW - M 809.

18. ALLEN, F. R., HAMMOND, A. D. The SGHWR version of the Monte Carlo code W-MONTE. AEEW - M 1158.

19. BEHRENS, D. J. The Effect of Holes in a Reacting Material on the Passage of Neutrons. Proc Phys Soc 62 607 1949.

Synthetic Geometry Approximations (see also Reference 2)

20. ASKEW, J. R. Some boundary condition problem arising in the application of collision probability methods. p 343 'Numerical Reactor Calculations'. IAEA 1972.

Integral Validation of Lattice Calculations (see also References 12 and 21).

22. CHAWLA, R. Improvements in the prediction of reactivity and reaction rate ratios for Uranium lattices. Jour. Nucl. Energy 27 797, 1973.

23. ASKEW, J. R., FAYERS, F. J., FOX, W. N. Thermal reactor temperature coefficient studies in the UK. AEEW - R 886.

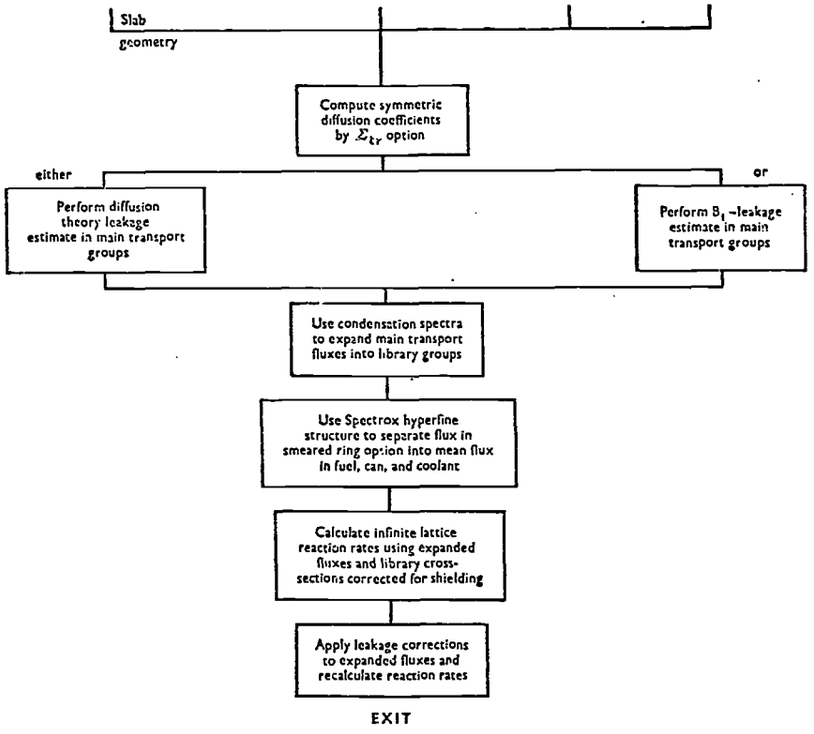

FIG. 1. Block diagram of computational sequences in WIMS

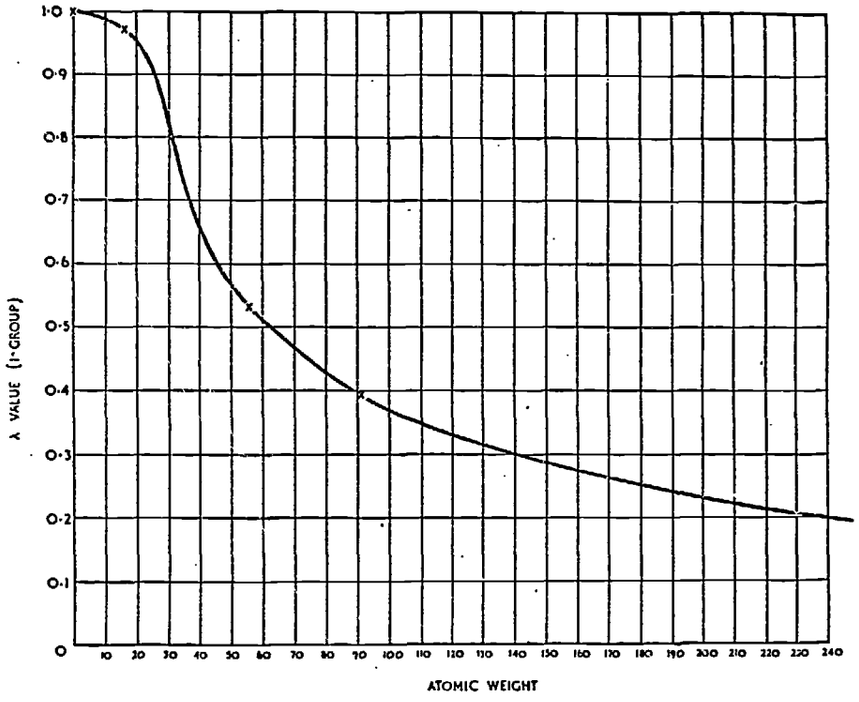

FIG. 2. GRAPH OF λ (1-GROUP) AGAINST ATOMIC WEIGHT

238 *Resonance captures in WIMS normalized to one neutron slowing down past the top of the appropriate resonance region*

Resonance regions:
5·53 keV to 4 eV for comparison with MOCUP
75·5 eV to 4 eV for comparison with SDR
1 keV to 0·625 eV for comparison with REPETITIOUS

Lattice description	Method of calculation		
	WIMS	MOCUP	SDR
Light water and 3% UO_2 regular rod array. Volume ratio 1:1	0·2121	0·2105 ±0·0018	
As above	0·1527	0·1495 ±0·0013	0·1528
Light water and 3% UO_2 regular rod array. Volume ratio 3:1	0·09027	0·0878 ±0·0013	
Light water and 3% UO_2 regular rod array. Volume ratio 4:1	0·07240	0·0685 ±0·0011	
As above	0·05197	0·0480 ±0·0008	0·04958
Heavy water and 3% UO_2 regular rod array. Volume ratio 4:1	0·3350	0·3345 ±0·0007	
37 rod cluster of 0·9% UO_2 rods. Light water cooled, heavy water moderated	0·1302	0·1255 ±0·0006	
37 rod cluster of 0·9% UO_2 rods. Air cooled, heavy water moderated	0·1727	0·1733 ±0·0013	
Light water and 1·3% metal regular rod array. Volume ratio 1:1	0·2885	0·2843 ±0·0021	
Light water and 1·3% metal regular rod array. Volume ratio 1·5:1	0·1999	0·1948 ±0·0025	
Graphite and 0·7% metal regular rod array. Volume ratio 30:1	0·2017	0·2000 ±0·0026	
U^{238}/H regular slab array. $N(238)\,t_f = 0.008489$, $N(H)t_m = 0.048506$	0·1055		0·1051
U^{238}/H regular slab array. $N(238)\,t_f = 0.092472$, $N(H)t_m = 0.007705$	0·1866		0·1874
U^{238}/H regular slab array. $N(238)\,t_f = 0.009391$, $N(H)t_m = 0.007705$	0·3294		0·3302 REPETITIOUS*
11·48 cm diameter U^{238}/H rod (N_a=0·009905 N_H=0·02469) in a sea of heavy water	0·1736	0·1747 ±0·0009	
As above	0·1685	0·1688 ±0·0010	0·1694
11·48 cm diameter U^{238}/H rod (N_a=0·009905 N_H=0·00777) in a sea of heavy water	0·1737		0·1696
11·48 cm diameter U^{238} rod (N_a=0·009905) in a sea of heavy water	0·1613		0·1550

* Repetitious results were kindly communicated by Dr R. L. Hellens of B.N.L. The Repetitious results are not expected to be in close agreement due to minor data differences and use of a flat source at 1 keV.

FIG. 3.

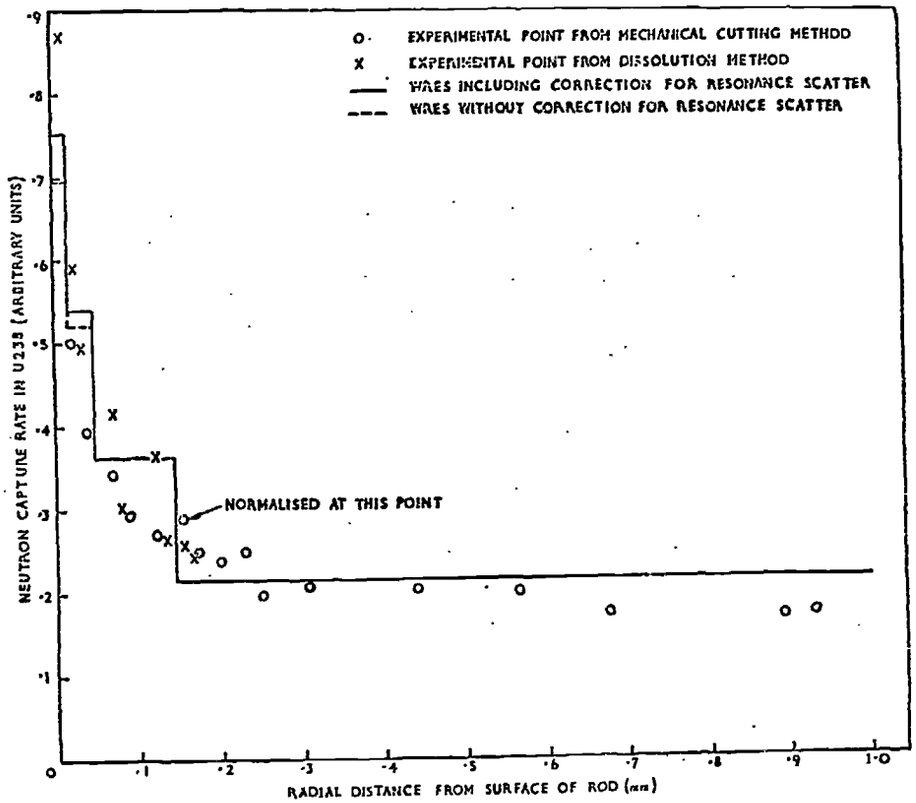

FIG. 4.

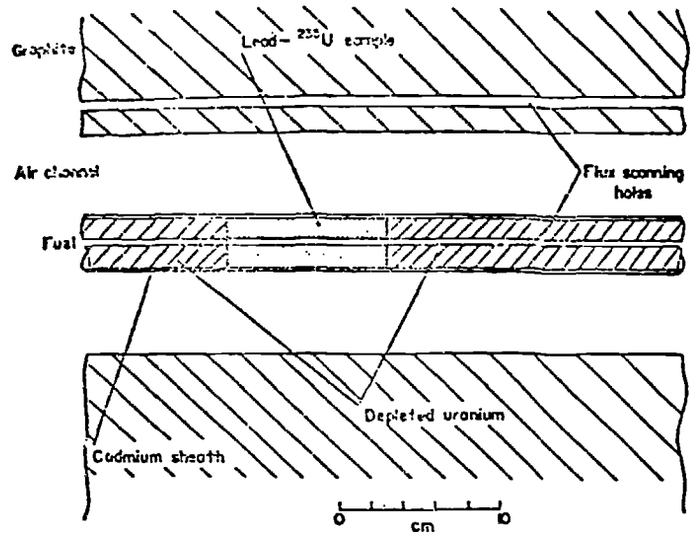

FIG. 5. Experimental Arrangement in Measuring Cell

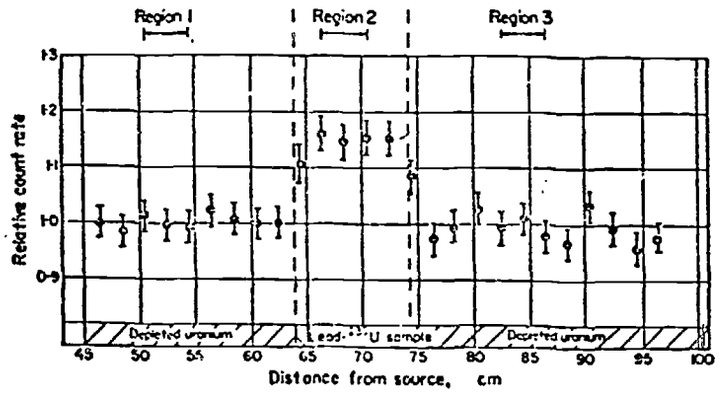

FIG. 6. –^{235}U fission chamber scan with 10-cm lead/^{235}U sample.

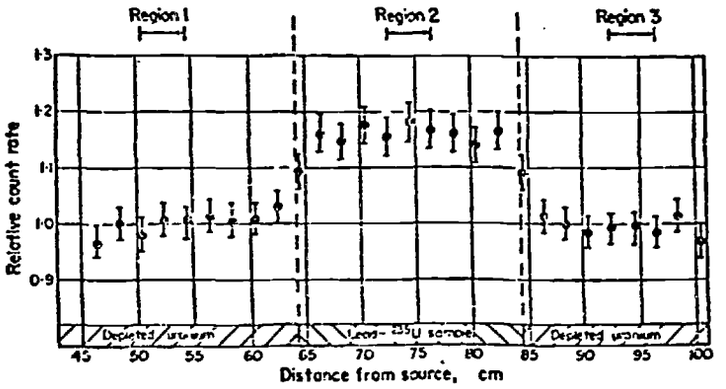

FIG. 7. –^{235}U fission chamber scan with 20-cm lead/^{235}U sample.

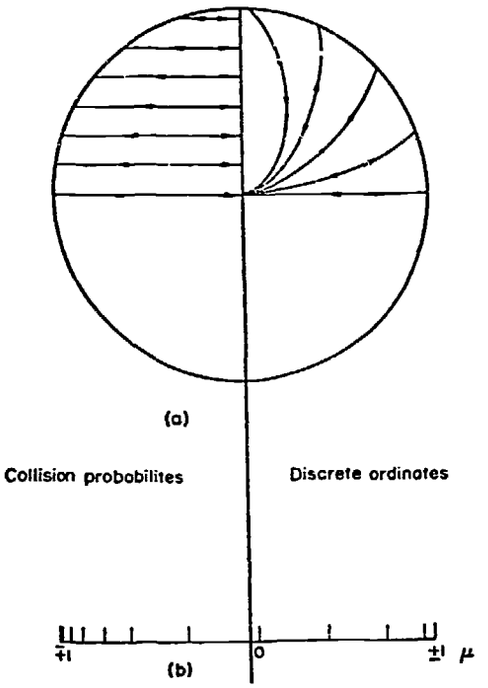

FIG. 8. (a) Typical tracking schemes for collision probabilities discrete ordinates. (b) Angular representations at outer surface. Collision probability and discrete ordinate tracking schemes in curved geometry.

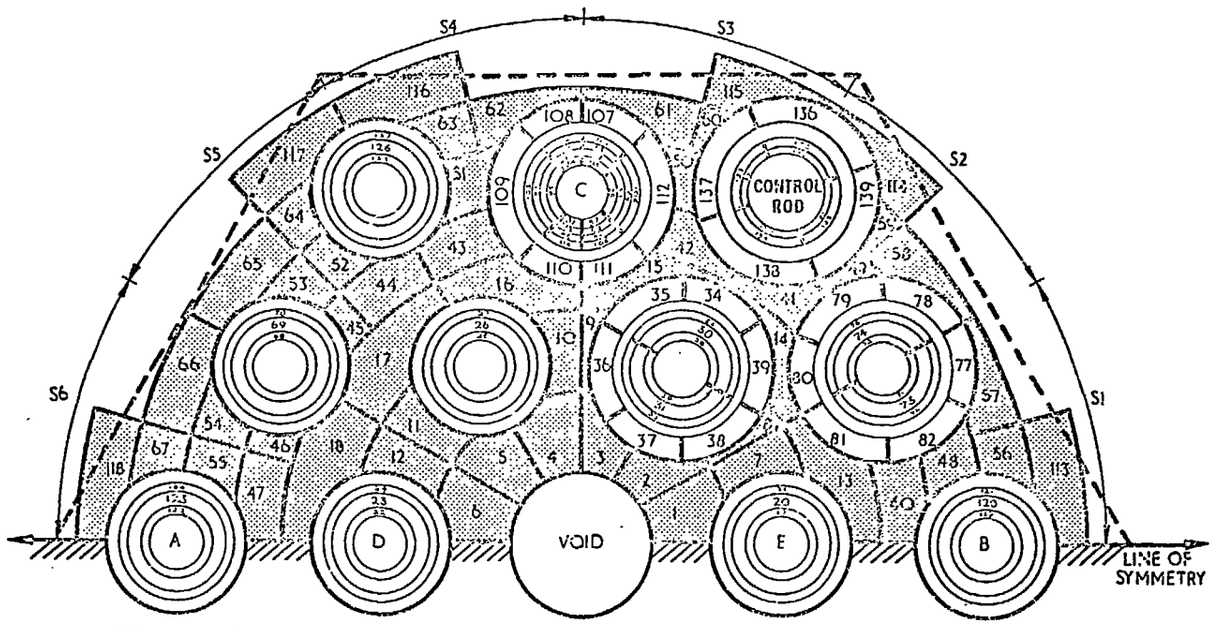

FIG. 9. ZENITH CENTRAL BLOCK SUB-DIVIDED INTO 139 REGIONS FOR PIJ CALCULATIONS.

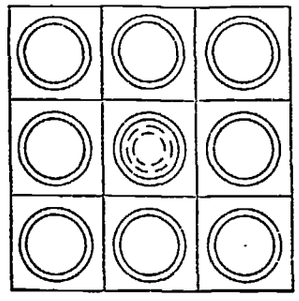

FIG. 10.

BURNABLE POISON SUPERCELL PROBLEM (PROBLEM 1)

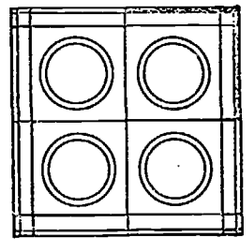

FIG. 11.

'MINI-BWR' PROBLEM WITH DIFFERENTIAL ENRICHMENT AND CRUCIFORM ABSORBER (PROBLEM 2)

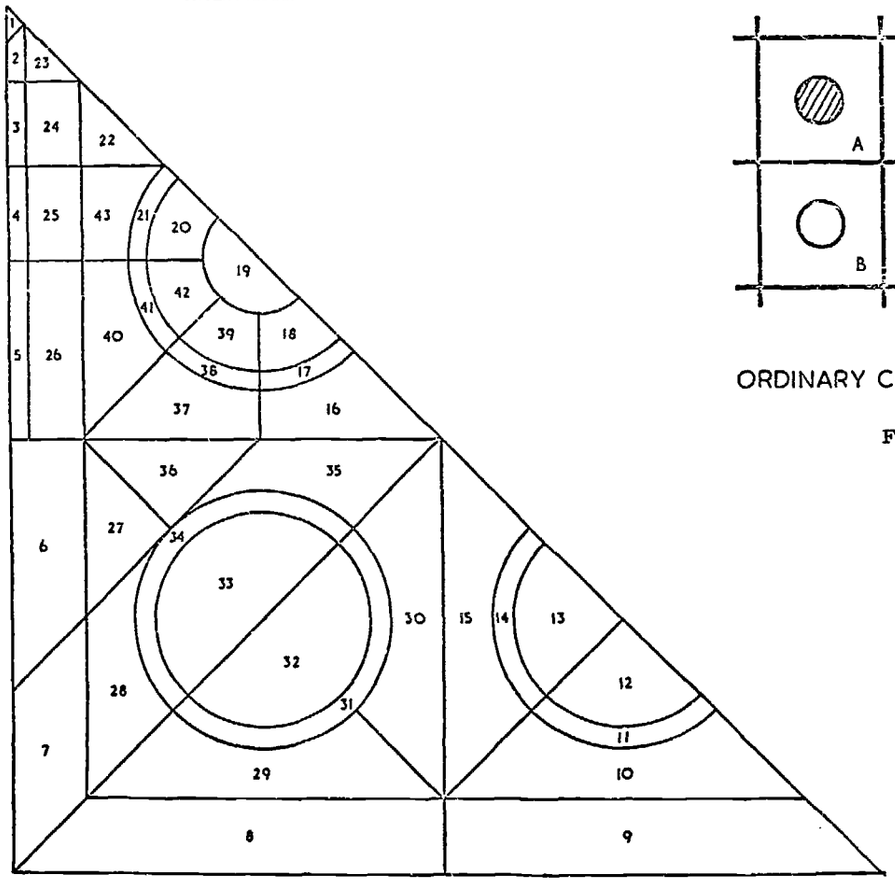

REGIONS USED IN THE 'BRISTOL' CALCULATION FOR PROBLEM 2

FIG. 12.

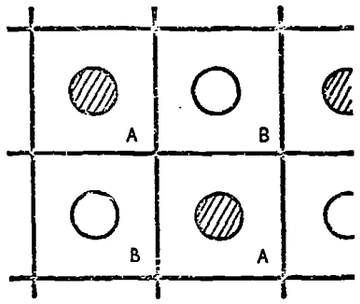

ORDINARY CHEQUERBOARD

FIG. 13.

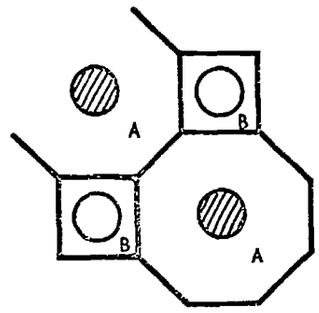

'ZERO CURRENT' CHEQUERBOARD

FIG. 14.

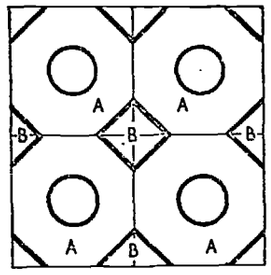

REGULAR LATTICE IN A CHEQUERBOARD APPROXIMATION

FIG. 15.

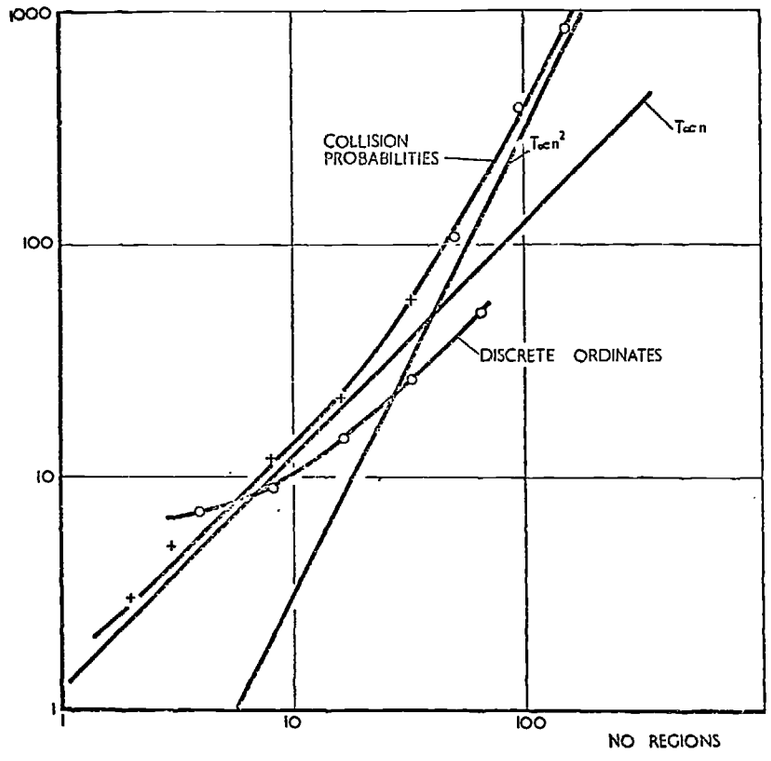

VARIATION OF COST OF SOLUTION WITH NUMBER OF REGIONS

FIG. 16.

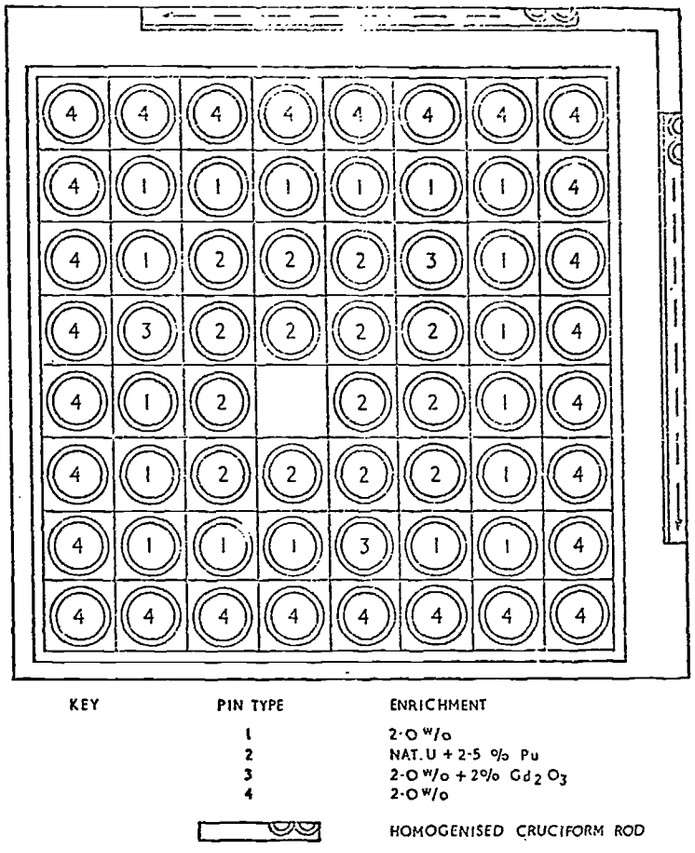

BWR LATTICE CELL WITH URANIUM, PLUTONIUM AND POISONED PINS. ONE EMPTY PIN POSITION AND A CRUCIFORM ROD (PROBLEM 4)

FIG. 17.

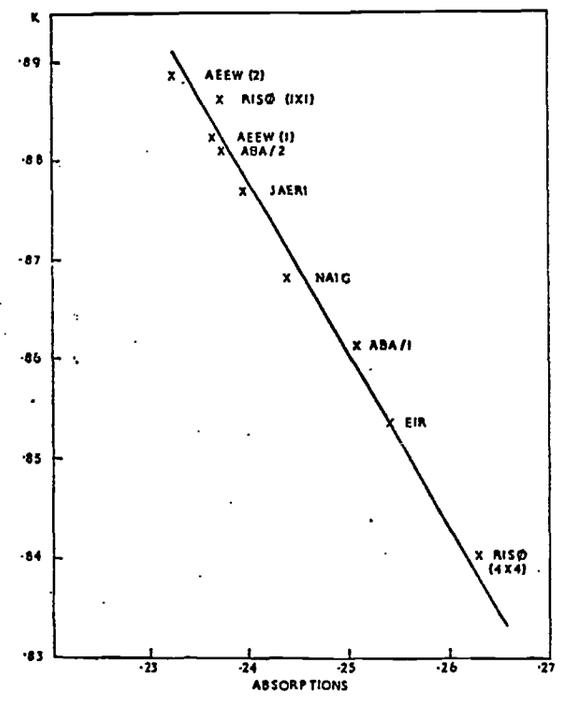

EIGENVALUE VS ABSORPTIONS IN POISON PIN
(PROBLEM 1)

FIG. 18.

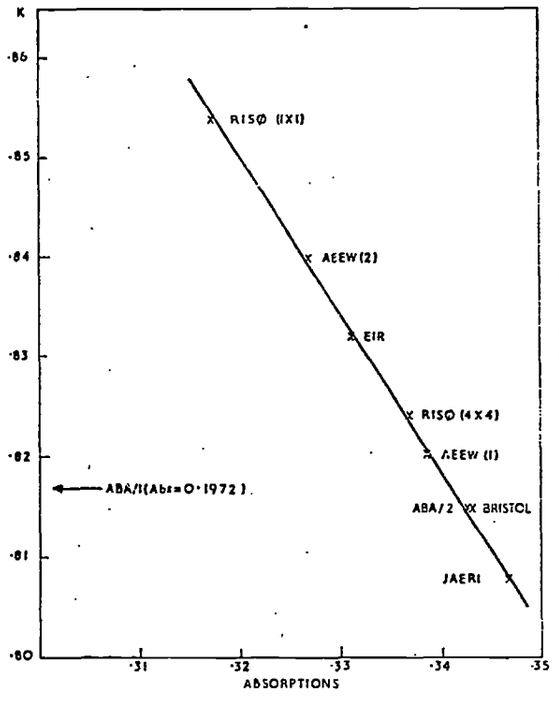

EIGENVALUE VS ABSORPTIONS IN CRUCIFORM ROD
(PROBLEM 2)

FIG. 19.

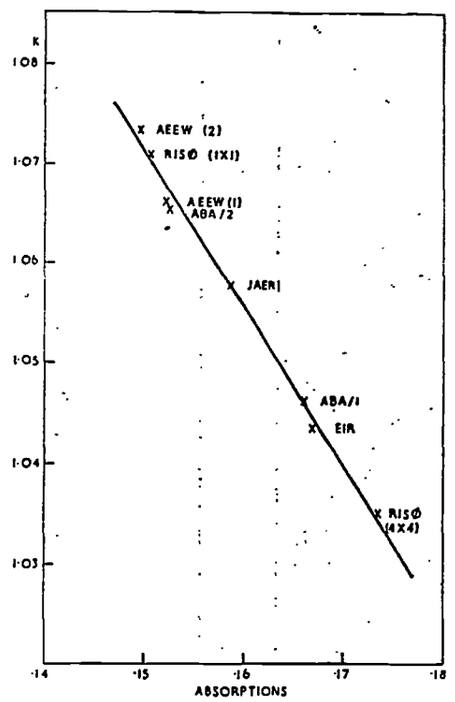

EIGENVALUE VS ABSORPTIONS
IN POISON PINS
(PROBLEM 3)

FIG. 20.

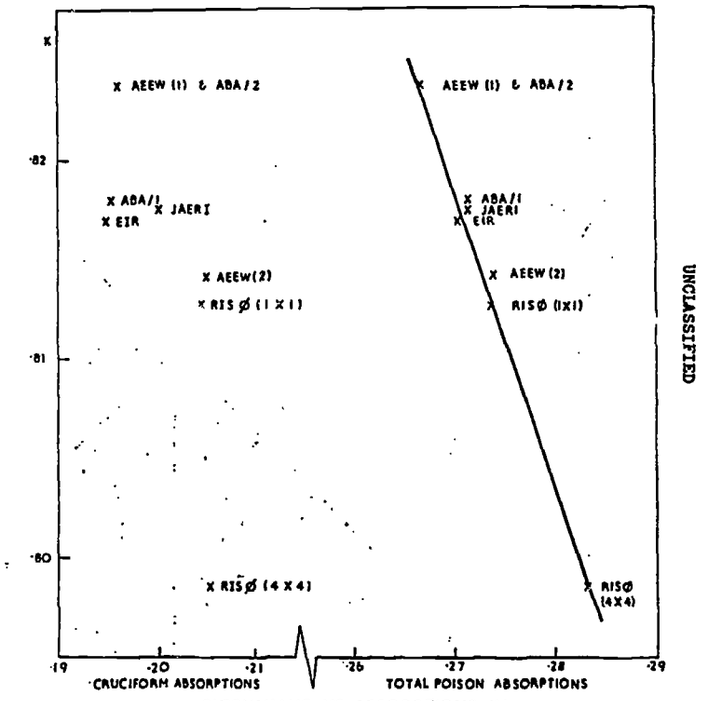

FIG. 21. EIGENVALUE VS ABSORPTIONS IN CRUCIFORM AND POISON PINS (PROBLEM 4)

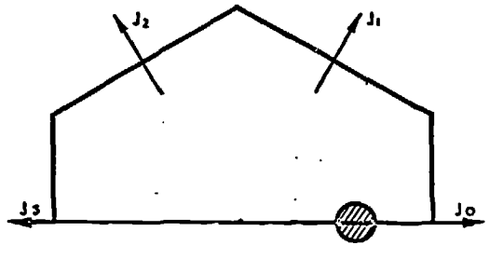

FIG. 22. BOUNDARY CONDITION FOR ASYMMETRIC ZONE

FIG. 23.

Thermal Absorption and Fission Cross-Sections and Resonance Absorption and Fission Integrals

Isotope	Identifier	2200 m/sec Cross-Section		Resonance Integral 0.55 eV – 2 MeV	
		Absorption	Fission	Absorption	Fission
Hydrogen	2001	0.332	–	0.140	–
Deuterium	8002	0.00056	–	0.00056	–
Boron	10/1010	3809.0	–	1667	–
Carbon	12	0.00340	–	0.00143	–
Oxygen	16	0.00009	–	0.00001	–
Aluminium	27	0.229	–	0.181	–
Silicon	29	0.160	–	0.0669	–
Chromium	52	3.10^{2}	–	1.33	–
Manganese	55	13.8	–	13.4	–
Iron	56	2.53	–	1.21	–
"Iron"	1056	2.53	–	2.61	–
Stainless Steel 304	9056	2.90	–	1.69	–
Nickel	58	4.60	–	2.04	–
Inconel 750X	8058	4.14	–	1.92	–
Inconel 718	9058	3.85	–	1.80	–
Zirconium	91	0.183	–	0.891	–
Zircaloy	9091	0.195	–	0.883	–
Silver *	2109	64.8	–	334	–
Cadmium	2113	2400	–	37	–
Indium	2115	202	–	3215	–
Gadolinium-155	2155	60050	–	1316	–
Gadolinium-157	2157	254000	–	493	–
Uranium-235 *	235	680	580	412	361
Uranium-236 *	236	6.08	0.0	313	0.517
Uranium-238 *	2238	2.72	0.0	272	0.180
Uranium-238 *	3238	2.72	0.0	273	0.181
Neptunium-239	939	65.0	–	17.6	–
Plutonium-239 *	2239	1029	742	446	262
Plutonium-240 †	1240	283	0.046	7625/7735	3.44
Plutonium-241	241	1387	1031	749	560
Plutonium-242	242	17.3	–	1043	–
Americium-241	941	625	–	1640	–
Americium-242m	942	8500	6800	2300	1840
Americium-243	943	94	–	1483	–
1/v absorber	1000	1.0	–	0.429	–

*These isotopes have resonance cross-sections tabulated as a function of temperature and σ_p; the infinite dilution integrals are quoted in this table.

†The absorption integral varies over the quoted range with a temperature range of 300°k to 1200°k.

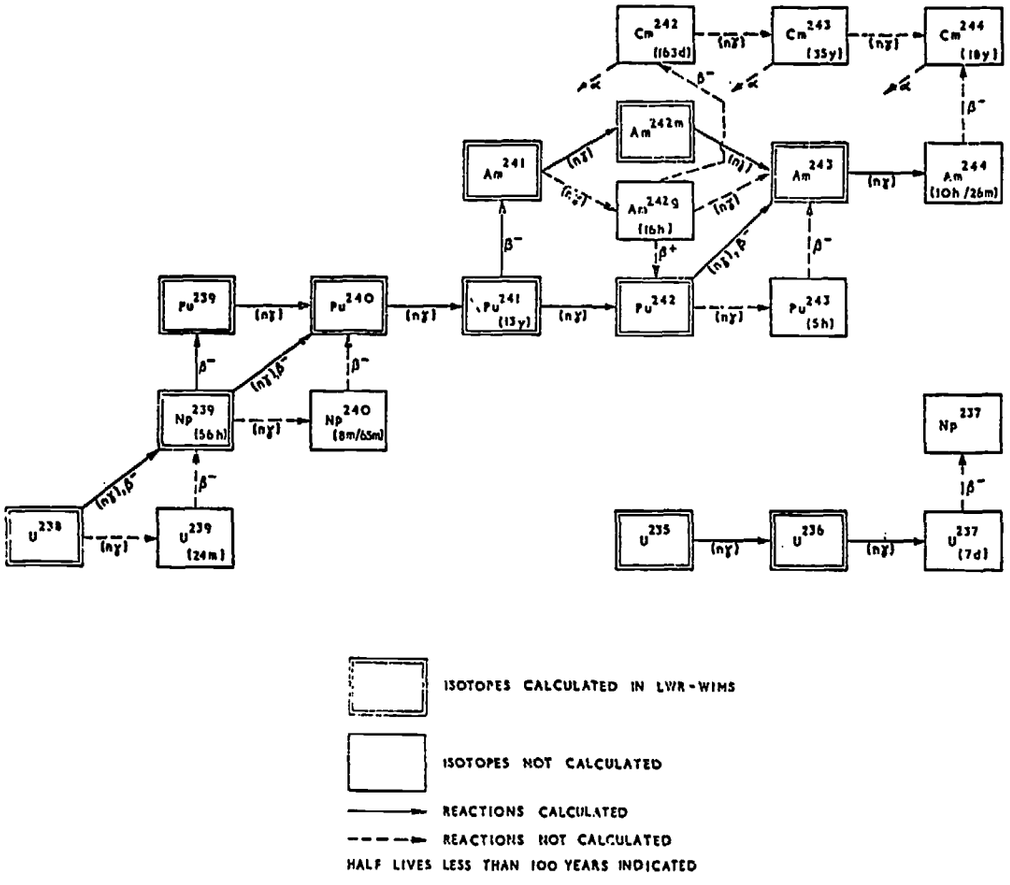

FIG. 24. PRINCIPAL LINKS IN THE HEAVY ATOM BURNUP CHAINS

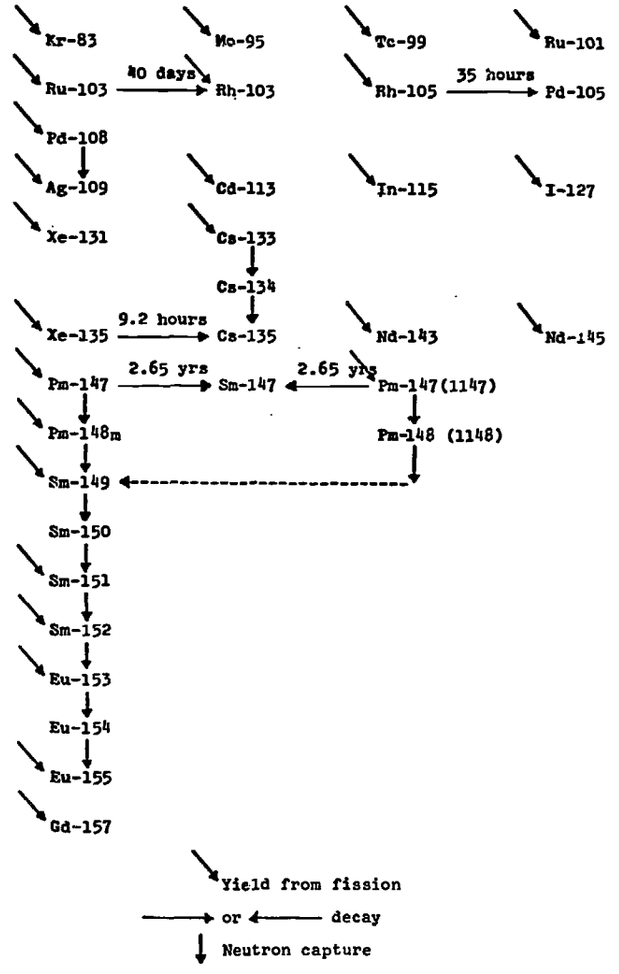

FIG. 25. FISSION PRODUCT CHAINS IN WIMS LIBRARY

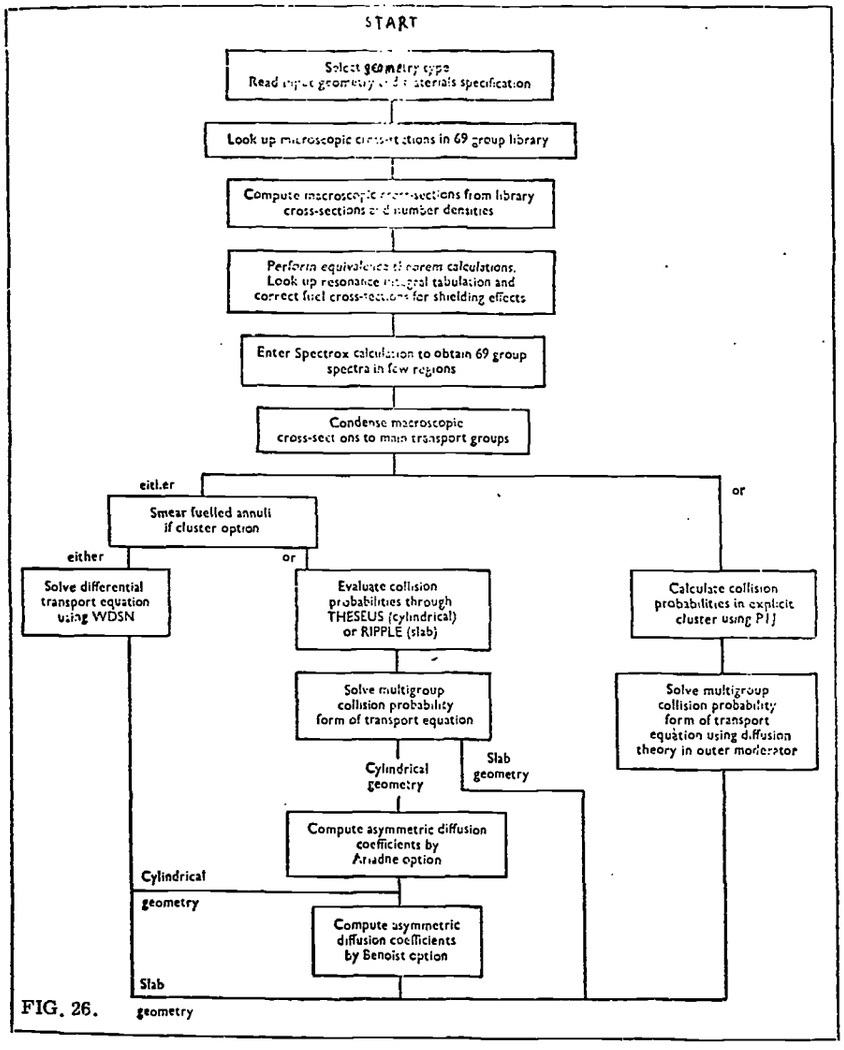

FIG. 26.

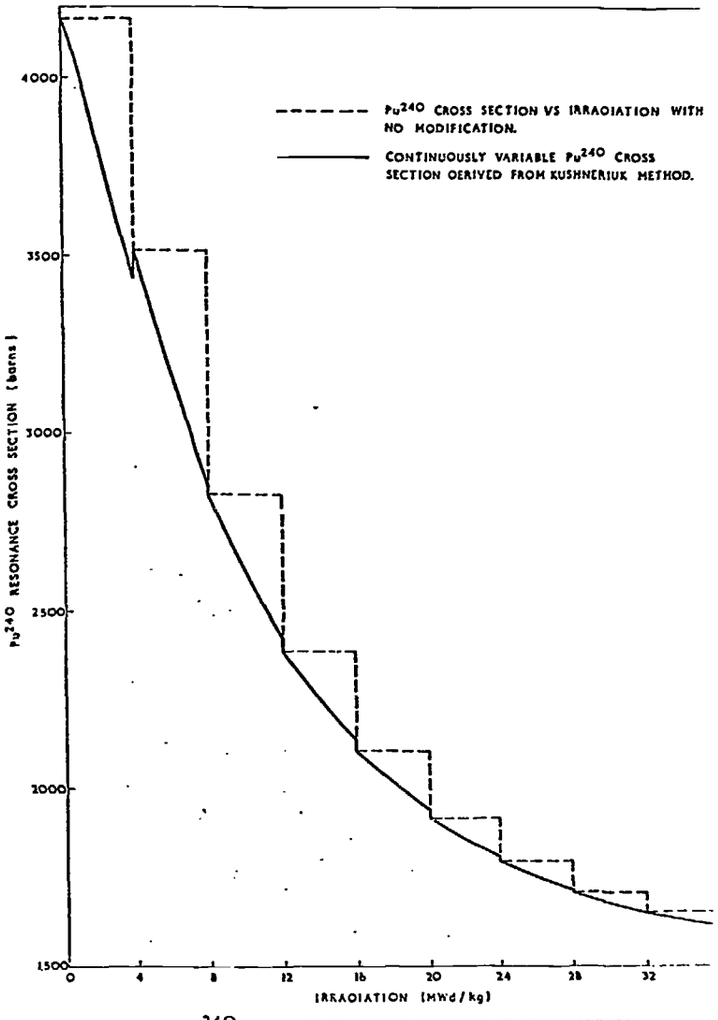

FIG. 27 Pu^{240} RESONANCE CROSS SECTION VS IRRADIATION